

SOME STUDIES IN THE FUNDAMENTAL PARAMETERS
OF FATIGUE

Thesis by
Sitaram Rao Valluri

In Partial Fulfillment of the Requirements
For the Degree of
Doctor of Philosophy

California Institute of Technology
Pasadena, California

1954

ACKNOWLEDGEMENTS

Many are the persons to whom the author is deeply thankful for the help he has received while working on his thesis. In particular, he would like to mention Drs. Y. C. Fung, E. E. Sechler, and D. E. Hudson for their suggestions and Dr. P. Duwez who was kind enough to look at the results and offer some extremely helpful suggestions. The author feels a deep sense of gratitude towards Dr. Sechler, whose encouragement and help in all directions exceeded the borderland of student-professor relationship. The author also owes many thanks to Dr. Fung for continuously striving to instill a spirit of preciseness and perfection.

The experimental work would have been impossible without the unstinting help of Mr. M. E. Jessey of the Electronics Section. Thanks are also due to Mr. C. A. Bartsch, Chief of the Machine Shop, for his support in building the equipment.

In the preparation of the thesis, the author gratefully acknowledges the help of Mrs. Virginia Boughton, Mrs. Elizabeth Fox, and Mr. and Mrs. Milton J. Wood.

ABSTRACT

A torsional fatigue testing machine of the resonant vibrator type has been designed in order to investigate the fatigue and internal friction properties of 3S-O aluminum. This machine uses an elastic restraint on an a-c motor to create resonant conditions and uses a photo-cell electronic system for the measurement of internal friction by the method of measuring the logarithmic decrement of free oscillations.

It has been established that for 3S-O aluminum at torsion stress levels below 112 psi, the stress history does not affect damping and that, for an annealed specimen, the material exhibits a maximum value of internal friction at 375°F. "Temporary mobility" aspects of the slip bands have been investigated and in addition, variation of internal friction as a function of stress amplitude in repeated torsional loading, temperature, and number of reversals has been obtained. At room temperature (75°F) the internal friction increases with the number of stress reversals in the 0 to 10^5 range. This increment in general increases with increasing amplitude of stress. At test temperatures of 225° and 525°F it was found that this increment does not show any regular variation with stress. In addition, however, it was found that at 375°F the internal friction decreases with stress reversals in the 0 to 10^5 range for all stresses. The variation of internal friction with stress history after a large number of stress reversals of the order 10^6 cycles, is quite complex, giving rise to random patterns of increase and decrease.

This work is exploratory in nature and suggestions for further work are indicated.

TABLE OF CONTENTS

PART		PAGE
	Acknowledgements	i
	Abstract	ii
	Table of Contents	iii
	List of Figures	v
I.	INTRODUCTION	1
II.	A BRIEF REVIEW OF PRIOR WORK AND A DISCUSSION OF THE NATURE OF SLIP AND GRAIN BOUNDARY	3
	a. Straining in a Single Crystal	3
	b. Straining of a Polycrystalline Aggregate	4
	c. Suggested Models of Grain Boundary	5
	d. Similarities between Grain Boundary Material and the Material in a Slip Band	6
	e. Temporary Mobility Aspects of the Slip Bands	7
	f. Influence of Temperature	8
	g. Prior Work Done to Correlate Fatigue and Damping	9
III.	SCOPE AND SPECIFIC OBJECTIVES OF THE PRESENT WORK	10
	a. Problems under Investigation	11
	b. Sequence of Experiments	12
IV.	CHOICE OF TEST MATERIAL	13
V.	TEST EQUIPMENT	15
	a. Design Considerations	15
	b. Design and Description of the Equipment	16
	c. Method of Decay Measurements	23
VI.	MEASURING TECHNIQUES AND ESTIMATION OF ERRORS	25
VII.	RESULTS OF TESTS AND DISCUSSION	31
	a. Determination of the Stress Level Below Which the Test Specimen is not Influenced by Stress History	31
	b. Determination of δ Vs. T. Relation	32
	c. Recovery Phenomena	33
	d. Discussion of Trends in Damping-Fatigue Relations	39
VIII.	SUMMARY OF RESULTS OBTAINED	45

TABLE OF CONTENTS (Continued)

PART		PAGE
IX.	A CRITICISM OF TECHNIQUES AND RECOMMENDATIONS	48
	References	51
	Tables	53
	Figures	69

LIST OF FIGURES

FIGURE		PAGE
1	Schematic Diagram of Vibrator	69
2a	Details of Flexure Pivot	69
2b	Closeup of the Inertia Bar and Details of Flexure Pivot	70
3	General View of the Test Equipment	70
4	Schematic Diagram of Test Set-up	71
5	Closeup of the Vibrator with the Test Specimen Mounted	72
6	General View of the Vibrator with its Accessory Equipment	72
7	Block Diagram for Measuring Circuit	73
8	Block Diagram for Power Supply to the Vibrator	73
9	Principle of Decay Measurements	74
10	Decay Measuring Equipment	75
11	Damping Curves for 3S-O Aluminum in Torsion	76
12	Variation of Internal Friction with Temperature	76
13	Variation of Recovery Factor with Temperature for Various Parametric Values of Stress	77
14	Variation of Recovery Factor with Stress for Various Parametric Values of Temperature	77
15	Recovery in a Typical Case as a Function of Non-dimensional Time	77
16	Fatigue-damping Curves for Test Temperature 75°	78
17	" " " " " 225°	79
18	" " " " " 375°	80
19	" " " " " 525°	81

LIST OF FIGURES (Cont'd)

FIGURE		PAGE
20	Fatigue-Damping Curves for Stress Level 2000 psi	82
21	" " " " " " 3500 psi	83
22	" " " " " " 5000 psi	84
23	" " " " " " 6000 psi	85
24	Variation of δ with T after Application of Fatigue Stress 3500 psi	86
25	Variation of δ with T after Application of Fatigue Stress 2000 psi	86
26	Variation of δ with T after Application of Fatigue Stress 6000 psi	87
27	Variation of δ with T after Application of Fatigue Stress 5000 psi	87
28	Reproduction of Fig. 16 with Scatter Band	88

I. INTRODUCTION

Members which are apparently in good condition, when subjected to repeated loading, have a tendency to break even though the applied load is substantially smaller than the normal breaking load under static conditions. Failures of this type are commonly denoted as "Fatigue Failures". A large amount of research, both fundamental and applied, has been conducted in order to ascertain the basic phenomena involved in fatigue failures. The problem is complicated by the number of controllable and uncontrollable variables which influence the start of fatigue failures.

Basic research by Gough, and others (Ref. 1) showed conclusively that fatigue failure is associated with the failure of "primitive elasticity" by the process of slip. Here the word "primitive" denotes that exhibited on the first loading. It has also been shown by them that the two events, namely: fatigue failure, and failure of primitive elasticity by the process of slip, are not simultaneous and that slip can occur at stress levels far below those associated with fatigue failures. It has been known for a long time that the phenomenon of slip gives rise to many other characteristics such as (a) internal friction, (b) stress and strain relaxation, (c) creep, etc.

Since both fatigue failures and internal friction find their origin in those regions of a metallic substance which also exhibit properties other than perfect elasticity, it has always been a tempting problem in research to determine if they can be correlated, either directly or with the help of some other physical variables which influence them. This has been

necessarily complicated because of a lack of proper knowledge of the physical variables involved in the problem or, if known, due to the difficulty in controlling these variables. This has resulted in a recent mushroom growth of papers in this field, often conflicting, if not directly contradictory.

The following work attempts to determine if there is any possibility of correlating, under controlled conditions, the amplitude of repeated stress, the number of cycles of reversals, the testing temperature, and the damping characteristics of the test material. The present work is primarily intended to investigate the trends which may need further exhaustive study.

II. A BRIEF REVIEW OF PRIOR WORK AND A DISCUSSION OF THE NATURE OF SLIP AND GRAIN BOUNDARY

Before the problem and its specific objectives to be investigated are stated, it seems worthwhile to discuss briefly the phenomenon of straining of a metallic member subjected to an external load.

a. Straining in a Single Crystal

A single crystal is built up of a number of unit cells arranged together in such a manner that a regular pattern is repeated throughout the crystal. If, for example, a pure shearing load is applied to such a metallic crystal, the crystal lattice will first deform elastically (in accordance with the generalized Hooke's Law); straining but not disrupting the interatomic bonds. If the straining action is increased in intensity, by increasing the external load, a limiting elastic strain will be exceeded and comparatively large movements will take place in the crystal along certain crystallographic planes in certain well-defined directions. Experiments by Taylor, Elam (Refs. 2 and 3) and others show that this movement occurs by the movement of lamellae of the crystal over one another. This movement in general is concentrated in a series of consecutive planes or thin sheets of the crystal. It has also been shown that these relatively large movements in crystal occur generally along those planes on which the atomic density is a relative maximum and in the direction of maximum resolved shear stress on these planes. These planes are defined as slip planes; the slip plane and the direction of movement, the slip direction, constitute a slip system. Various theories have been proposed to explain this property

of slip exhibited by physical crystals. Of these, the most important is the dislocation theory suggested and developed by Orowan (Ref. 4), Polanyi (Ref. 5), Taylor (Ref. 6), and others. Briefly, this assumes that these crystals have certain imperfections, which can move and be created by external forces. Cumulative effect of such movements will be revealed as slip. This theory is known as the dislocation theory of slip and recent experiments tend to support this theory.

b. Straining of a Polycrystalline Aggregate

In a polycrystalline aggregate, however, the problem is complicated by the grain boundaries. These grain boundaries are brought into existence as a consequence of the simultaneous development of the solid state from a molten mass from various randomly disposed nuclei. Each one of these small individual crystals which constitutes the major part of the metallic aggregate is of the same physical structure as the single crystal described above.

If a specimen made of this polycrystalline aggregate is subjected to a similar straining pattern as that applied to one made of a single crystal, the slip phenomena occur in the individual crystalline grains, with the difference that not all of them experience slip simultaneously and that this slip movement is influenced by the grain boundaries which surround the crystals. Those favorably situated are subjected to slip movement first.

The property of solids in which stress and strain are not uniquely related, but is elastic in the sense that a body returns, asymptotically, to its initial unstressed configuration after the removal of all external

stress, is called "anelasticity" by Zener (Ref. 7). However, in the crystalline aggregate, one has to face the problem of grain boundaries. Unfortunately, because of the order of magnitude involved, no direct investigation of the grain boundary material properties has been possible to date. In general, its properties have been ascertained by conducting experiments with single crystals and the polycrystalline aggregate of the same material. It has been found in general (Refs. 1, 8, 9, 10) that a grain boundary inhibits slip, that a crack does not follow a grain boundary, that it behaves as a viscous material in energy dissipation, that it is of a different phase from the rest of the material as indicated by density differences between single crystals and crystalline aggregate and that, in some metals at least, it is stronger than the crystal itself.

c. Suggested Models of Grain Boundary

Various theories have been proposed to explain the structure of the material in the grain boundary. Of these, two have received wide attention. They are Rosenhain's amorphous theory (Refs. 11, 12), and a second which imagines a transition region at the boundary, where the atom positions represent a compromise between the crystalline arrangements in the two adjoining grains. Rosenhain's theory imagines that the boundary consists of an undercooled liquid whose assumed properties are entirely in accordance with the known properties of the boundary. Metallurgists have been reluctant to accept the concept of amorphous phase since no metallic material has been produced mechanically in that phase. Zener (Ref. 7) points out that "no controversy need

arise, once it is realized that it is not necessary for any portion of the material to be in amorphous phase in order that the grain boundaries may behave in a viscous manner. It is necessary only to assume that the resistance to slipping of one grain over an adjacent grain obeys laws commonly associated with amorphous materials rather than laws associated with crystalline materials". He further argues that, since the surface atoms of one grain cannot fit into the lattice position of an adjacent grain, the binding across an interface may be assumed to be amorphous in nature. It is interesting to note that this explanation does not pretend to give a model of the grain boundary but takes the attitude that it is of no great consequence as to what is the exact picture of the grain boundary so long as we can reasonably ascertain its physical properties.

d. Similarities Between the Grain Boundary Material and the Material in a Slip Band

It has already been mentioned that the grain boundary material exhibits certain properties which are not associated usually with crystalline materials. We also have this condition produced to a certain extent by the process of slip. As it is observed under a microscope, the tell-tale traces of slip on the surface of a specimen are not the consequence of a single slip movement alone, but a series of movements in adjacent planes. These concentrated regions of slip movement are commonly designated as slip bands. One question that immediately comes up relates to the nature of the material in the slip band. This seems to be of fundamental importance since it has been

found that the initiation of a crack in fatigue failure in general takes place in a region previously overworked by the slip process, though the macroscopic propagation of this crack may well depend on the nature of the stress field in the region.

Physical characteristics of the material as a whole suggest that the effect of slip is something more than the observed relative movements in some planes of the crystal. There is strong evidence already available that, at least temporarily the material in a previously formed slip band is viscous in nature (Ref. 7, p. 133). It is also found that the material gets strain hardened as a whole, that having been formed once, a slip band in some metals, such as aluminum, resists further slip along the same bands (Refs. 2, 13). One may note that this inhibition of slip is also shown by the grain boundary material. Consequently, there is some reason to suspect that the material in the grain boundary and slip bands may be similar in nature.

e. Temporary Mobility Features of the Slip Bands

A series of tests conducted by Lord Kelvin deserve attention. He showed that sustained vibrations on thin wires in torsion substantially increase the damping capacity of specimens as compared to those that were not subjected to the same stress history. He also showed from his tests that a period of rest has a tendency to reduce this increment of damping capacity of the specimens. It has already been mentioned that there is some evidence available towards the possibility of the material in the slip bands being temporarily viscous in nature and then gradually resuming the elastic state. It seems plausible then, that the

recovery (decrease) of damping noticed by Kelvin may be due to this temporary mobile nature of the slip bands. If this were to be so, then it is reasonable to expect that the damping immediately after a period of forced vibration should be a function of time, and as the concept of the temporary mobile nature of slip suggests, should result in a decrease in damping after a time as compared with a value found immediately after stopping the forced vibrations. It is implicitly assumed here that an increase in damping exhibited by a material subjected to forced vibration is primarily due to the slip bands and that this damping is due to the temporarily viscous nature of the slip bands. It is apparent, in accordance with this concept, that as the slip bands acquire an elastic state their capacity to dissipate energy in damping should decrease and hence should result in a decrease in damping.

f. Influence of Temperature

The influence of temperature on fatigue and grain boundary damping has received much attention. It has been known that fatigue life is substantially lowered by an increase in temperature. Kê's experiments showed conclusively (Ref. 10, and others) the influence of temperature on the grain boundaries. He conducted tests on specimens of pure aluminum in polycrystalline aggregates over a wide range of grain sizes and showed that there exists a critical temperature at which the internal friction of the specimens is a maximum. By a simple reasoning he argues that this is the behavior of a viscous grain boundary. It is apparent that at this critical temperature, at which the internal friction of the grain boundaries is a maximum, the energy dissipation

capacity of the material is also a maximum. Since fatigue failure requires absorption of energy, it is interesting to inquire if the critical temperature for internal friction is related to the fatigue strength. Another tantalizing question that arises is, "Is it possible to estimate the fatigue life, say at room temperature, by a process of extrapolation if the life of the material is known at higher temperatures?". This also will be of some practical importance since it can conceivably reduce the time of fatigue testing.

g. Prior Work Done to Correlate Fatigue and Damping

In the work conducted recently by Lazan and his associates (Refs. 16, 17, 18, 19) definite attempts have been made to correlate fatigue, damping and temperature. Their technique involved the measurement of damping by the phase lag method in rotating bending cantilever machines especially designed for this work. Their measurements of damping observed under stress on carefully prepared specimens showed the existence of what is called the "Cyclic Stress Sensitivity Limit; C.S.S.L.". This is a stress level below which the damping capacity of a specimen subjected to repeated loading is not altered within the limits of experimental error. They also found that in the lower range of stress above C.S.S.L. the variation of specific damping energy with stress satisfies the equation

$$D = JS^n$$

where D is the specific damping capacity, S is the stress level and, J and n are constants depending upon the material. According to them, cyclic stress below approximately 80 percent of the fatigue limit has relatively small effect on damping and "dynamic modulus of elasticity",

whereas stress applied between the C.S.S.L. and fatigue limit increased damping by as much as 2500 percent and reduced the "dynamic modulus" by as much as 11 percent. They also found that the damping of a metallic member is very much dependent upon the previous stress history, temperature and operating stress level. They noticed various interesting and unexplainable patterns and "depending on the material and temperature, the damping may increase, decrease or have a complex pattern of increase and decrease". They found no regular behavior for all materials, and changes of substantial magnitude were found to take place above and below the fatigue strength as defined by a value of stress level needed to produce failure with 20×10^6 cycles.

It must be pointed out that in Lazan's work, the damping is measured at the stress level of the forced vibrations, which, in general is above the C.S.S.L. A major part of this damping arises from the plastic deformation of the material and does not reveal the purely anelastic properties of the specimen.

In the following work conducted at the Guggenheim Aeronautical Laboratory of the California Institute of Technology, the damping is determined by the logarithmic decrement method, where the specimen is not simultaneously subjected to the stress of forced vibrations at a stress level higher than the C.S.S.L. This, it is felt, is necessary in order that one may measure only that part of the damping that the test specimen retains and exhibits under low stress level vibrations.

III. SCOPE AND SPECIFIC OBJECTIVES OF THE PRESENT WORK

This work is an investigation of the behavior of commercially pure 3S-O aluminum under fatigue loading in torsion at various temperatures and the determination of damping under the same conditions in an effort to correlate these two parameters.

a. Problems Under Investigation

Briefly, the questions that are kept in mind in this work are:

(1) Investigation of the trends in the variation of internal friction as measured by the logarithmic decrement δ as a function of torsional shear stress τ , temperature T , number of reversals N .

(2) Influence of periods of rest on damping of the test specimens under the same conditions.

(3) Does an estimate of the internal friction at various temperatures and stress levels offer a means of predicting fatigue life?

(4) Determination of the critical temperature for the viscous behavior of the grain boundary material and its possible relation to the fatigue problem.

(5) Checking the temporarily viscous nature of the slip bands by determining the variation of δ as a function of time after subjecting the test specimens to periods of vibration at various temperatures and stress levels.

(6) Determination of the highest stress level below which the test specimen can be excited in free vibrations in order that these vibrations do not influence the stress history of the specimen as indicated by variation of δ . This part is dictated by necessity in order to avoid

extraneous stress history on the test specimens and hence was one of the first to be determined.

b. Sequence of Experiments

In order to investigate the above, the following sequence of experiments is found desirable.

(1) Determination of the highest stress level below which the damping of an annealed specimen is not affected by the stress history.

(2) Determination of the variation of internal friction δ as a function of temperature T , for an annealed specimen from room temperature up to the maximum obtainable in the furnace.

(3) Determination of the internal friction δ as a function of stress τ , temperature T , and cycles N .

(4) Determination of the variation of δ as a function of time in the series of tests suggested in (3) in order to determine the temporary mobility aspects of the slip bands.

Tests (3) and (4) above are made simultaneously as will be observed later on.

IV. CHOICE OF TEST MATERIAL

Having decided the scope and sequence of the experiments, it appeared worthwhile proceeding with a pure metal, preferably aluminum. One of the reasons is, some sort of information about the experiments suggested in (2) above is already available from Kê's work, and second, in order to avoid high textural stresses (Ref. 20) in the metal, test specimens in substantially pure form are considered desirable. Since it is desired to investigate the effect of slip on internal friction, it is necessary to have a controlled stress history for all the specimens. This is achieved by subjecting all the specimens (chosen from the same stock) to the same annealing conditions.

Commercially pure 3S-O aluminum in the form of 1/8 inch diameter wires, 36 inches long were obtained locally. Each of these wires is held vertically with a load of approximately 750 psi acting in tension and a current of 175 amperes at 30 volts is passed initially for a period of 10 minutes. This raises the temperature of the wire to about 750°F and substantially straightens the wire. Three pieces, each of length 9 inches are cut from each of the 36-inch long wires subjected to the above treatment. These are used as test specimens after subjecting them to further annealing in the furnace mounted on the testing machine. Due to the high ductility of the test material, great difficulty is experienced in keeping the test specimens straight while mounting them in the machine. It is because of this that it has become necessary to anneal the specimens after mounting them in the machine. In addition, methods have been adopted to keep the specimens straight while mounting and throughout the test.

The aluminum wires, as obtained locally, have reasonably good surface polish and no special effort is made to improve upon them. However, each specimen is checked carefully for scratches, nicks and similar surface imperfections. After finally mounting in the machine, each one of the test specimens, which has 6 inches of free length, is heated up to a temperature of 650°F and kept at that temperature for 8 hours and gradually brought down to the "room temperature" which has been kept at $75^{\circ} \pm 3^{\circ}\text{F}$. Its internal friction is determined at this stage and if this value is less than a value chosen in a manner to be described later, the specimen is rejected and a different specimen is tried.

V. TEST EQUIPMENT

a. Design Considerations

The design of equipment and instrumentation has posed some special problems. It is felt that they have to satisfy the following requirements.

- (1) Damping be measurable in a short period of time.
- (2) Damping measurements be easily repeatable.
- (3) The test equipment be made as flexible as possible in order to enable easy changes.
- (4) Design should be such that variable frequencies of operation are available.

The photographic method of determining the damping is not considered feasible because of the time element, and the cumbersomeness of determining δ , and the additional human errors involved in the method. "Width of the resonance curve" method is not found possible since in the setup conceived, there is an additional member in the form of an elastic restraint for creating resonant conditions and energy is dissipated both in the specimen as well as in the restraint. Finally, since it is desired to measure the damping at low stress levels as previously described, free oscillations in torsion, coupled with a photo-cell and electronic system was decided as the best means under the existing conditions. This method which is described in detail later, has one disadvantage in that the complete damping curve usually obtainable in the optical-photographic system, is not obtainable except with slightly involved techniques. But considering the extreme ease with which

damping can be measured by this method, it is felt worth sacrificing the above advantage of the optical-photographic system. Since only one machine is contemplated, it has become necessary to use a relatively high frequency in order that results may be obtained in a reasonable period of time. It was finally decided to use approximately 350 cps as the operating frequency.

Mechanical setups consisting of cams and four bar linkages were tried and rejected as unsuitable due to mechanical difficulties. Finally an electrical system of the resonant type has been adopted. In the preliminary tests it was found that if an elastic restraint is attached to one end of a 2-pole a-c motor as shown in Fig. 1, and a current passed through the coils on the poles, it is possible to excite torsional vibrations in the rotor provided the angle θ is not zero. By choosing a proper length for the restraint, it is possible to create a resonant condition in the system and thus maintain oscillations of substantial amplitude with little power input. The frequency of oscillation obtained actually is double the frequency of power input. This principle is utilized with some refinements. The final setup is shown schematically in Fig. 4. The photograph in Fig. 3 shows all the equipment used in this work.

b. Design and Description of the Equipment

Referring to Figs. 4, 5, and 6 "1" is the resonant type vibrator whose 2-pole stator is built up of silicon steel laminations with pole faces of dimensions 1 inch by 1-1/2 inches. The vibrator whose details are given in Fig. 1 B is mounted on a 3/8-inch cold-rolled steel shaft. This also is built up of silicon steel laminations and solid dural

pieces in the form of segments of cylinders are used to form the short-circuited secondary of the rotor. The stator housing accommodates bearings through which the vibrator shaft passes and is held in position. To the upper end of the shaft is connected an elastic restraint (3/8-inch diameter drill rod). The upper end of the elastic restraint is held rigid by means of the vise "20". "13" are the blower fans to keep the vibrator cool. The saturation value of the poles of the vibrator is approximately 200 volt-amperes.

To the lower end of the vibrator shaft is attached a mirror holder "3" which indicates the amplitude of the forced vibrations with the help of the light source "19" and the amplitude scale "18". The distance between the amplitude scale and the mirror holder is adjusted such that each inch of amplitude corresponds to 1000 psi of torsional shear stress on the surface of the test specimen.

To the bottom of the mirror holder is fixed the extension rod "4". The other end of this extension rod holds the specimen with the help of collets. To the other end of the specimen is attached another extension rod "6", identical with "4". To the lower end of the extension rod "6" is fixed the inertia bar "7" made of dural with cold-rolled end pieces. Facing these end pieces are the electromagnets "8" connected so that they induce a torsional couple when excited by a d-c current. The electromagnets are carried on the yoke "22" held in any desired angular position in the horizontal plane by the vise "10".

Just at the top of the inertia bar is the slit mirror "11"(1/32-inch by 1/2 - inch) intended for decay measurements in free vibration. The end of the extension rod "6" projecting beyond the inertia bar is held in

position by the flexure pivot "9".

Item "14" is the furnace enclosing the test specimen and is controlled by the iron-constantan thermocouple located very near the specimen. In order to control the temperature gradient inside the furnace within $\pm 5^{\circ}\text{F}$ heating elements "15" are installed. These elements and the main elements are controlled by powerstats and power transformers mounted on the panel "21". "12" is the outlet for pressure regulated compressed air to blow on the extension rod just below the mirror holder while the furnace is working. This acts as a heat insulator between the hot and cold parts of the setup. It is found that due to the natural gradient, no such arrangement is necessary at the bottom. This part remains at room temperature.

The whole system is mounted on the I-beam "16", which is 5 inches wide and 5 inches deep and has its front face planed in order to facilitate proper alignment of the various parts. The vibrator, furnaces, vises, etc. are held in position by 3/8-inch diameter Allen screws with conical ends working against the machined and inclined backface. The I-beam is held in a vertical position in the frame "17" supported on three studs with spherical surfaces working in hemispherical holes of three steel plates. Alignment of the whole setup is effected by means of a plumb line hanging from the bottom of the mirror holder and pointing against a sharp-pointed rod pointing upwards from a hole inside the vertical central rod of the yoke piece "22".

The weight of the inertia bar and the extension rod "6" are the direct axial loads on the test specimen and this amounts to an axial tension of 112 psi.

The ratio of the frequency of forced vibration to the natural vibration of the test specimen is of the order 100 to 1 and consequently no special restraint is found necessary to keep the inertia bar end of the test specimen stationary in order to create a fixed end condition in forced vibrations.

Because of great difficulty experienced in keeping the test specimen vertical (in order to induce only torsional stress) some sort of support at the bottom of the inertia bar was found necessary. Various methods have been tried, such as critical viscous damping; thin piano wire kept in tension at the end of the inertia bar; a .032 inch diameter drill rod working in a miniature precision bearing; a conical pivot; and finally, a flexure pivot. Of all the methods tried, from the point of view of least amount of friction, piano wire and flexure pivot are found to be the best. Thus, for example, for a particular amplitude decay, the conical pivot, dashpot in viscous damping, miniature precision bearing, piano wire, flexure pivot with unsoldered ends, and flexure pivot with soldered end gave respectively 30, 150, 320, 600, 650, and 700 cycles. Piano wire has certain advantages over the flexure pivot in design but due to the difficulty experienced in keeping the axial tension low and constant it has finally been decided to use the flexure pivot.

In this connection the work of W. H. Wittrick was helpful. He showed (Ref. 21) that if the flexures cross at 87.3 percent of the free length instead of at the center, then the instantaneous center of rotation remains fixed to a high order of accuracy and the restoring torque vs. the angle of rotation is linear up to almost 45° . In this work, the angle of rotation is hardly $1/4^{\circ}$. To facilitate minor adjustments, the flexure

pivot is mounted such that small amounts of both horizontal and vertical movements are available. Details of the design finally incorporated are indicated in Figs. 2 A and 2 B.

Since the elastic restraint is also subjected to torsional vibrations it is necessary to design it in such a manner that it does not fail in operation. Also, its dimensions have to be such that it will have the correct amount of stiffness to obtain the desired resonant conditions. This can be done conveniently as follows:

Let D be the diameter of the elastic restraint

K be the torsional stiffness

L be the length of the restraint

θ be the maximum angular movement in torsional vibration

M_T is the applied torque

I_p is the polar moment of inertia of the cross section

τ is the shear stress

r is the radius = $\frac{D}{2}$

G is the rigidity modulus

Following the torsion theory for uniform circular cylinders we have the relation

$$\frac{M_T}{I_p} = \frac{\tau}{r} = \frac{G\theta}{L} \quad (1)$$

From the definition of K , we have,

$$K = \frac{M_T}{\theta} = \frac{GI_p}{L} \quad \text{or} \quad \frac{G}{L} = \frac{K}{I_p} \quad (2)$$

Substituting this in Eq. (1) and simplifying, we get

$$\tau = \frac{16 K D \theta}{\pi D^4} = \frac{16 K \theta}{\pi D^3} \quad (3)$$

The endurance limit for the drill rod material used as an elastic restraint is 40,000 psi in torsion. In a preliminary test intended to check the behavior of the machine, an elastic restraint 7 inches long and 3/16 inch diameter was used and this gave a resonant frequency of 59.3 cps.

The stiffness for this case from Eq. (2) is

$$K = 10 \times 10^6 \times \frac{\pi}{32} \times \left(\frac{3}{16}\right)^4 \times \frac{1}{7} = 179 \text{ inch-lbs with } G = 10 \times 10^6 \text{ psi}$$

As a first approximation we can use $\omega_n = \sqrt{\frac{K}{m}}$ for the natural frequency of the system.

$$\text{Then, we have the equivalent mass } m = \frac{K}{\omega_n^2} = \frac{179}{(59.3)^2} \text{ slugs.}$$

\therefore m is known from this preliminary test.

Suppose now we want a natural frequency of 2 x 175 cps. Then the required $K = m \omega_n^2 = \frac{179}{(59.3)^2} \times (175)^2 = 1550 \text{ lb-inches}$. For the final design of the restraint, therefore, we are given the endurance limit of the material τ , and the maximum angular displacement θ . It is desired to get the length L and the diameter D to satisfy the above conditions.

θ maximum on the basis of 8000 psi maximum shear stress in the test specimen amounts to roughly 0.25 radians.

$$\text{From Eq. (3) } D^3 = \frac{16 K \theta}{\pi} = \frac{16 \times 1550 \times 0.25}{\pi \times 40,000} = 0.0493$$

whence we get $D = 0.366 \text{ in} \approx 3/8 \text{ in}$.

It was consequently decided to choose 3/8 in. diameter drill rod as the elastic restraint. The length of the restraint is obtained from

the equation

$$L = \frac{G I_p}{K} = \frac{10 \times 10^6}{1550} \times \frac{\pi}{32} \times \left(\frac{3}{8}\right)^4 = 12.5 \text{ in.}$$

These calculated values of length L and diameter D checked within 1 cps the theoretical value of 175 cps for resonance condition.

Due to core saturation and the friction in the system it was found that at this frequency of 350 cps the maximum amplitude obtainable is not more than 6500 psi of maximum shear stress on the test specimen. Due to the extreme service conditions it has been found necessary to change the bearings in every 100 million cycles of operation.

A close-up view of the specimen mounted on the machine is shown in Fig. 5. In order to develop a uniform pressure around the test specimen at the ends where it is mounted into the extension rods, collets made of cold rolled steel are used. These are held inside the enlarged end of the extension rod by means of a pair of screws. This method is found to be quite effective.

The power supply to drive the vibrator is obtained by means of an audio oscillator and a 250 watt amplifier. The system is shown schematically in Fig. 8. The parallel connection from the audio oscillator to the events per unit time (Eput) channel of the Berkeley counter is intended to check the accuracy of the oscillator output frequency.

Because of the extreme softness of the aluminum specimens used in this work, great difficulty has been experienced in keeping the specimen straight while mounting. Methods have been devised in order to overcome this difficulty.

Energizing and de-energizing of the electromagnets, in order to

start the specimen impulsively in free oscillation, is accomplished by means of a control panel with relay equipment located near the counter.

c. Method of Decay Measurements

The measurement of amplitude decay, which is a measure of damping, is accomplished as shown schematically in Fig. 9. When the inertia bar is stationary and the specimen is in an unstrained condition, the incident light from the light source L is reflected by the slit mirror to the position Z on the scale S. OZ' is the bisector of the angle LOZ and the angle LOZ' represents the zero angle. If now the electromagnets are energized, the inertia bar and hence the specimen is deflected from its zero position, the reflected light occupies the position M. LOM' is the actual deflection angle and the strain in the specimen is represented by the angle Z'OM'. Now, when the electromagnets are de-energized, the specimen is started impulsively from the position M and executes free torsional vibrations. The damping of the system gradually damps down the oscillation. At P is a slit 1/64 in. x 1 in. and behind it is a photocell. Every time the light beam crosses the slit in its free vibration the photocell receives and sends a signal to an amplifier and this is used to actuate an electronic counter. Since the vibrations are damped down continuously, after a while the reflected light does not quite reach the slit. Since the counter counts all signals up to this stage and since we know the zero position and maximum amplitude position and photocell position, we can calculate the damping from the formula

$$\begin{aligned}\delta &= \frac{2}{n} (\text{Log}_e M'OZ' - \text{Log}_e P'OZ') \\ &= \frac{2}{n} (\text{Log}_e MZ - \text{Log}_e PZ)\end{aligned}$$

The number 2 above n is introduced since the counter counts half cycles. The derivation of the above formula and its implications are discussed in the estimation of errors.

In order to facilitate visual observations for adjustments and settings, the reflected ray of light in the form of a line 2 in. x 1/16 in. traverses the scale in such a manner that the upper half covers the slit in its travel and the lower half travels across the scale. The photocell and the light source are mounted on a table, movable in a vertical direction for adjustments to take care of the expansion of the test specimen with temperature (and hence a lowering of the slit mirror on the extension rod). In addition, the photocell is mounted on a traversing screw in order to help plotting of damping curves and the like.

The electrical system involved in the damping measurements is shown schematically in Fig. 7 and in the photograph in Fig. 10. The oscillograph is used in the circuit in order to monitor the signal from the amplifier and take care of noise level and threshold plate voltage of the photocell and discriminator adjustments. Duplicate connections from the output of the oscillograph to the period measurement channel of the Berkeley counter are used for measurements of period of the test specimen in free vibration.

VI. MEASURING TECHNIQUES AND ESTIMATION OF ERRORS

The validity of correlating the damping phenomena with the fatigue properties largely stems from the fact that both of them have their origin essentially in the same regions. Since damping is an indirect measure of certain things happening in the material, the changing damping values characterize, at any particular moment, the physical structure at that instant and under those conditions only. Consequently it is imperative that the conditions under which the damping of a member is being measured be also the conditions under which the other physical properties (such as fatigue) are also being measured.

There are many ways in which energy can be dissipated in a system under observation. These can be broadly divided into two categories:

- (1) External influences

- (2) Internal dissipation such as internal friction due to atomic movements in the grain boundary, slip bands, etc. This second class of dissipative mechanisms are in general difficult to isolate into its various parts except possibly under some special circumstances.

In this work there are five places where extraneous damping of the first kind can occur. They are,

- (1) The bearings at the ends of the vibrator

- (2) The grip between the collets and the specimen at the ends of test specimen.

- (3) The supporting mechanism at the bottom of the inertia bar whether it be flexure pivot or any other means.

- (4) Magnetic hysteresis due to possible stray magnetic fields.

(5) Aerodynamic damping due to the movement of the inertia bar in the air.

Every effort has been made to reduce the effect of the above items as much as possible.

The bearings at the ends of the vibrator did not contribute to the damping in free vibration to any extent. This is illustrated by the fact that no change was noticed in the value of δ for an annealed specimen, beyond small random variations, when the top extension rod was held rigid just below the bearings. Further in these damping tests, the angular movement at the bearings is of the order of 1/400th of one degree. In addition, since energy dissipation is proportional to the angular displacement, and since the displacement is small, this effect is neglected.

Determination of the friction at the collet grips is more difficult. No estimates or measurements seem to be possible. Before a particular test is started, the screws facing the collets in the extension rods are tightened as much as possible and checked again at the end of the test. Further, whenever suspected, the collets are changed in order to avoid friction losses in that vicinity. It is still possible that a certain amount exists here.

Maximum friction was observed at the bottom of the inertia bar where the bottom extension rod has to be supported in order to simulate pure torsional vibrations. For reasons already mentioned, flexure pivots were adopted. It should be noticed that when the ends of the flexures were properly fixed, the energy dissipation in them would be of the same nature as that of the test specimen itself with this difference:

that the amount of material and the order of stress involved were very small.

For starting the free vibrations of the test specimen impulsively, a pair of electromagnets and cold-rolled steel pole pieces on the inertia bar are used. For a long time, these were not suspected of giving rise to any appreciable dissipation of energy since it was assumed that the pole pieces and the cores of the electromagnets did not retain any residual magnetism. This assumption was found to be unjustified while determining the damping curves. Since this can conceivably affect the results, the electromagnets and the pole pieces were demagnetized from time to time. It was found that this boosted up the decay cycles from 700 to 800 at room temperature. In the latter stages of testing, it remained substantially constant at this level. It may be noted in this connection that at higher temperatures the internal damping is of a higher magnitude than this damping due to the residual magnetism and consequently influences the results to a lesser extent.

In regard to the aerodynamic damping, since the frequency of vibration in the damping tests is rather small (of the order of 3.5 cps) it is felt that its effect is negligible (Ref. 14).

A variation from the mean of as much as 13 percent is detected in the damping of the annealed specimens at room temperature.* This variation in damping is attributed to all of the above causes and it is suspected in addition that a major part of this is inherent in the material even after the annealing process.

* If a test specimen showed a variation by an amount larger than this from 750 cycles required normally for decay, the specimen was rejected and another one was tried.

While the above is the cumulative error in initial damping from specimen to specimen, errors of a different nature exist in measurements of damping of one specimen after various numbers of reversals. For example, it is found that when a specimen is annealed and its damping is measured, it is clearly statistical in nature with a variation of about ± 35 cycles in 700 cycles at room temperature in a typical case. The variations at higher temperatures are, in general, of a smaller order. When interpreting the results, this inherent random variation is kept in mind and only those variations of behavior which appreciably depart from these inherent variations are taken into account.

Still another type of error exists in the measurements and it has its source at the photocell. If x_1 and x_2 are a pair of adjacent amplitudes in free vibration with positive damping, then the ratio $\delta = \log_e \frac{x_1}{x_2}$ is a measure of the damping of the system. This ratio is commonly called "the logarithmic decrement". If we assume that the equivalent viscous damping is constant, then we have

$$\delta = \log_e \frac{x_1}{x_2} = \log_e \frac{x_2}{x_3} = \dots \log_e \frac{x_{n-1}}{x_n} ,$$

and hence

$$n \delta = (\log_e x_1 - \log_e x_n)$$

and

$$\delta = \frac{1}{n} (\log_e x_1 - \log_e x_n)$$

where x_1 is the amplitude at any instant and x_n is the amplitude after n number of cycles.

In the measuring technique used here, errors can be made in locating x_1 and x_n . It is consequently worthwhile estimating their

effect.

One can put the above equation in the form

$$n = K \log_e \frac{x}{x_n}$$

Now suppose in setting x , the starting amplitude of free vibration, an error Δx is made. The number of cycles would now be different and let it be $n + \Delta n$.

$$\text{Then } \Delta n = k(\log_e \frac{x + \Delta x}{x_n} - \log_e \frac{x}{x_n}) \approx K \frac{\Delta x}{x}$$

$$\text{therefore percent of variation} = 100 \frac{\Delta n}{n} = 100 \frac{K}{n} \times \frac{\Delta x}{x} = 100 \frac{\Delta x}{x \log_e \frac{x}{x_n}}$$

In a similar manner one can obtain the error in the number of cycles, when an error of Δx_n is made in x_n . This would be the case if the slit in front of the photocell is not located accurately. This amounts to

$$100 \frac{\Delta x_n}{x_n} \frac{1}{\log_e \frac{x}{x_n}} \text{ percent. The maximum possible errors in setting}$$

$$\text{are } \Delta x = \frac{1}{40} \text{ in. and } \Delta x_n = \frac{1}{100} \text{ in. and } x = 1 \text{ in. } x_n = 0.4 \text{ in.}$$

Therefore error in setting x is 2.7 percent I

and, error in setting x_n is 2.7 percent II

Since it is conceivable that errors of the first kind can be committed in the initial zero setting, it is apparent that this has to be added twice. In order to cut down the errors of the second kind, the photocell location (and hence x_n) is kept constant throughout this series of tests and we have consequently a total error of $2 \times 2.7 = 5.4$ percent.

Thus to recall,

(1) When comparing results from one specimen with the other, there is a variation of initial damping up to ± 13 percent.

(2) In the measurement of damping of a specimen there is an

inherent statistical variation in the damping of about 5 percent in range about the mean value. While looking for significant trends, this has been taken into account and only variations which depart from this have been considered.

(3) There is a maximum error of 5.54 percent in the measurement of damping from reading to reading of a specimen between a number of reversals of forced vibration.

As a consequence of the heavy feedback employed in the amplifier circuits, the amplitude of forced vibration does not fluctuate to any great extent. This was found to be, in general, less than 4 percent except when the specimen was about to break.

The temperature in the furnace which has been calibrated does not vary beyond $\pm 5^{\circ}\text{F}$ maximum in the temperature range of 75° to 650°F .

The inherent scatter exhibited by all problems of fatigue makes a statistical analysis imperative. In this connection, the work of Epremian, Mehl, and others (Refs. 22 and 23) showing that scatter exists not only in fatigue life, but also in the determination of the endurance limit, is of fundamental importance. Whenever there seems to be any possibility to determine fatigue life or endurance limit by short cuts, one has always to bear in mind this inherent scatter in fatigue problems, and remember that the results are more likely to be represented in graphs by bands rather than lines.

* It may be mentioned here, that while calibrating the furnace, thermocouples were installed directly on the test specimen. The main thermocouple near the specimen and the powerstats controlling the auxiliary heating elements were calibrated against these thermocouples directly. The temperature variations given above refer to these thermocouples on the test specimen.

VII. RESULTS OF TESTS AND DISCUSSION

In the following, for purposes of identification of the test specimens, the notation τ - T - N is adopted. This signifies that the amplitude of repeated loading is τ psi in torsion on the outermost fibers of the test specimen; the test temperature is T, and N is the number of the test specimen with the above two test variables. Thus, for example, 2000 - 75 - 1 indicates that the annealed specimen is subjected to a stress of 2000 psi in torsion at a temperature of 75⁰F and that this is the first specimen with these two test variables.

The number of cycles in free vibration required for a chosen amplitude decay is hereafter called "the decay cycles". These are the number of cycles required for the amplitude of 1 inch to die down to 0.4 inches on a linear scale at a distance of 130 inches. Since these amplitudes are kept constant, it is apparent $1/n$, where n is the decay cycles, is a measure of damping.*

a. Determination of the Stress Level Below which the Test Specimen is not Influenced in Damping by Stress History

Kê's work on grain boundary shows that damping for small oscillations is viscous and is not influenced by stress history. Elsewhere information is available to indicate that at high stresses, damping is influenced by the amplitude of stress. Consequently it is apparent that a stress level should exist below which stress history does not affect the damping of the specimens and the damping is due only to the grain boundaries.

* Substituting the values of MZ and PZ in the equation on page 24, one obtains $\delta = \frac{1.8326}{n}$. While plotting, $\frac{10^3}{n} = \frac{x \cdot 10^3}{1.8326} = 550 \times \delta$ is used as a measure of damping.

Considering the expression for damping, $\delta = \frac{1}{n} (\log_e x_1 - \log_e x_n)$, if one were to plot the damping curves for free vibration on a semilog paper, wherever the damping is constant, the slope of the curves would be constant. Therefore, in order to determine the maximum stress level below which the damping is constant, damping curves with various starting amplitudes are determined and plotted in Fig. 11. It is clear from these curves that below a stress level of 112 psi the slopes of all the curves are substantially constant and hence correspond to constant damping coefficient which is synonymous with viscous damping. The slightly different and higher slopes of the curves in the beginning are attributed to the effect of the electromagnets. In the subsequent tests, error due to this is not considered serious since it remains constant. Thus it has been established that below a stress level of 112 psi in torsion, the damping of 3S-O aluminum as indicated by the logarithmic decrement is constant and is not influenced by the stress history,

b. Determination of δ vs. T Relation

This test has to be performed in order that one may determine the critical temperature T_{cr} at which the value of δ is a maximum. This curve is presented in Fig. 12. As indicated by Kê, this curve has a maximum at a temperature of 375°F. It may be noticed that this temperature of 375°F is different from the value 536°F reported by Kê in his work. No definite explanation is offered for this variation except to mention that the materials tested are not quite the same. The aluminum specimens with which Kê worked were supplied by Alcoa, specially prepared for him, whereas in this work, the material is

obtained locally. It is possible that the difference in critical temperature is due to this.

In the subsequent tests, the variation of δ as a function of stress level τ , temperature T , and the number of reversals N is determined. Thus, after annealing the specimen, its damping is determined. Now a particular stress level τ , and temperature T are chosen and the damping values of the specimen are determined after various numbers of reversals N . This process is carried up to 30×10^6 cycles unless the specimen breaks within that period. While the damping is being determined, the test specimen is not subjected to forced vibrations and this period of time did not exceed 15 minutes in any instance.

Earlier work indicated that the torsional endurance limit of aluminum on the basis of 500×10^6 cycles is approximately 5000 psi. It is felt desirable to traverse through this range. Since 375°F is a critical temperature for the test material, it is felt desirable to traverse through this range also. Consequently the following stress levels and temperatures are chosen for investigation.

τ	2000	3500	5000	6000 psi
T	75°	225°	375°	525°F

c. Recovery Phenomena

While reviewing prior work, it has been suggested that the temporary mobility aspect of the slip bands may exhibit itself by an increase in the number of decay cycles (hence a reduction of damping capacity) if the readings are taken at intervals immediately after the

forced vibrations are stopped. In these tests this, indeed, is found to be the case. However, it is also found that this recovery is dependent on the stress level of forced vibrations and the temperature as well. It has also been found that under certain conditions, there occurs what one may call "negative recovery", wherein the decay cycles instead of increasing, decrease with time.

In order to analyze and present these phenomena, the following procedure is adopted.

The difference between the maximum and minimum readings for decay cycles for an annealed specimen is determined in all cases. This difference is also determined for the readings obtained in the measurement of damping after the specimen has been subjected to forced vibration. If this difference is larger than the corresponding difference for the same specimen at the same temperature but in an annealed condition, then this difference is considered significant. In addition it is considered significant only if there is noticed either a monotonic increase or decrease in a set of readings. Thus for example, considering the case 2000 - 75 - 1, the annealed specimen gave the following readings for the decay cycles: 669, 651, 649, 649, 652, 651, with an average of 654 and a difference between the maximum and minimum reading equal to $669 - 649 = 20$. Now for the same specimen, the decay cycles obtained after 46,500 cycles of forced vibrations are in order 451, 457, 478, 485, 492, and 520, with an average of 481 and a difference between the maximum and minimum of 69. The ratio of the first reading to the last largest reading in the series (in this case $\frac{520}{451} = 1.15$) is denoted as the "recovery factor". Since the difference

69 is larger than the corresponding difference 20 for the same specimen under annealed conditions, and since there is a monotonic increase, it is considered that this is a case of significant recovery. In cases where a monotonic decrease is noticed, it is apparent that would be the case of a recovery factor being less than 1 and for obvious reasons this case is designated "negative recovery". In order to represent graphically, cases where no significant recovery is noticed are assigned a recovery factor of 1.

To facilitate ready examination, the complete information for all the test specimens is presented in the tables 1 through 16. Column 1 in these tables denotes the number of cycles after which the decay cycles are recorded. In columns 2 through 7 are noted the decay cycles $n_1, n_2 \dots n_6$. Column 8 gives the average of n 's. Thus, $n_{ave} = n_1 + n_2 + n_3 + n_4 + n_5 + n_6 / 6$. Column 9 gives $1/n_{ave}$ and this is actually a measure of the damping since all other terms in the expression for the logarithmic decrement, δ , are constants. Column 10 gives the difference between the maximum and minimum readings in each row from n_1 to n_6 , both included. Column 11 gives the significant recovery factor in each case. One may obtain an idea of the time taken for these readings by knowing that the frequency of natural vibration is approximately 3.5 cps.

The recovery phenomena can be best analyzed from two points of view. In the first case, the stress is kept constant and the variation of recovery with temperature is discussed. In the second case, the temperature is kept constant and the variation of recovery with stress is discussed. Before either of these is done, the behavior of each

specimen is briefly discussed from the recovery point of view.

In the test specimen 2000 - 75 - 1, in 16 sets of readings, one can observe positive recovery in 9 cases, negative in 2 and no significant change in the remaining 5. No trend is noticeable in the variation of recovery factor with number of cycles of forced vibration. The average recovery factor for all the positive cases is 1.09.* No explanation is offered for the occurrence of the two cases of negative recovery within the first few minutes of operation.

For the test specimen 2000 - 225 - 1, in 15 sets of readings 13 indicated negative recovery, one positive, and one no trend. This is a complete change of trend as compared to the previous case. No trend is noticeable in the variation of recovery factor with the cycles of forced vibrations. The average recovery factor, which is negative in this case, is 0.95. The single positive recovery factor occurred in the first five minutes of running.

For the test specimen 2000 - 375 - 1, the recovery factor is predominantly negative. Thus in a set of 16 readings, 11 gave a negative recovery factor, one positive and four no trend. However, the single positive recovery factor and the four no-trend cases occurred in the first 30 minutes and from then on the recovery factor is consistently negative. The average negative recovery factor is 0.94, slightly smaller than the one for 2000 - 225 - 1.

For the test specimen 2000 - 525 - 1, no significant trend can be

* It may be observed in some cases that the scatter about the average recovery factor is rather appreciable. In the absence of sufficient data at this stage, it is considered desirable to work with these average recovery factors only.

noticed. Therefore the assigned value of the recovery factor is 1.

Looking at the four cases, one notices a change from a positive recovery factor to negative recovery factor with the increase of temperature and at higher temperatures there is an absence of recovery.

The trends in the specimens with stress level 3500 psi are somewhat different. For the test specimen 3500 - 75 - 1, in a set of 15 readings, 14 gave positive recovery factor and one no trend. The average positive recovery factor is 1.14 as compared to the corresponding value of 1.09 in 2000 - 75 - 1 case. The recovery factor did not show any orderly variation with the forced vibrations.

For the test specimen 3500 - 225 - 1, one notices no recovery in any of the readings. The assigned recovery factor is 1.

For the test specimen 3500 - 375 - 1 one notices two cases of positive recovery in a total of 13 sets of readings, and no negative recovery cases. Thus, this is predominantly a case of no recovery. The assigned recovery factor is 1.

For the test specimen 3500 - 525 - 1 again no recovery is noticeable. The assigned recovery factor is 1.

Looking at these four cases, it appears that the two cases of positive recovery noticed are freak. If this is accepted, it would mean that except for the room temperature case, recovery is absent at 3500 psi at the higher temperatures at which the specimens are tested.

For the test specimen 5000 - 75 - 1, out of 14 sets of readings, there is positive recovery in 11 cases, negative recovery in one case, and two of no trend. The average positive recovery factor is 1.15 - higher than the corresponding cases of 3500 - 75 - 1 and 2000 - 75 - 1.

For the test specimen 5000 - 225 - 1, out of 14 sets of readings 12 gave positive recovery, and two no trend. There are no cases of negative recovery and the average recovery factor is 1.08.

For the test specimens 5000 - 375 - 1 and 5000 - 525 - 1 no recovery is noticeable. The assigned recovery factor for each case is 1.

Looking at these four cases, one would notice that it is difficult to draw any conclusions regarding trends in the recovery factor except that there is a decrease in the recovery with increase of temperature.

Test specimen 6000 - 75 - 1 is a case of predominantly positive recovery, with an average recovery factor of 1.16. No explanation is offered for the single negative recovery factor occurring in this case.

For the test specimen 6000 - 225 - 1, of eight sets of readings five gave positive recovery factor, one negative, and two no trend. One notices something of a trend in the variation of recovery factor with cycles of forced vibration. There is a general increase up to the last but one reading. The average recovery factor is 1.17.

For the test specimen 6000 - 375 - 1, a total of eight sets of readings gave only one case of positive recovery and the assigned recovery factor for this case is 1.

There is no noticeable recovery for the test specimen 6000 - 525 - 1. The assigned recovery factor is 1.

The trends in the recovery factor as a function of temperature for various parametric values of stress based on the above analyses

are represented graphically in Fig. 13. Similarly by cross plotting, one can obtain the variation of the recovery factor with stress for various parametric values of temperature. This is shown by the curves in Fig. 14.

These curves indicate some interesting trends. For example, one notices that room temperature recovery factor increases with the increase of stress, at first rather rapidly and then more gradually with stress. At 225° the slope of recovery factor vs. stress is much steeper. No explanation is offered now for the negative recovery factor which occurs at 2000 psi at 225°F. At 375°F the specimens start with a negative recovery factor and with increase of stress reach and merge with the curve for recovery factor 1. At 525°F the curve is identical with the line for recovery factor 1.

If recovery phenomena find their origin in the slip bands, then it seems probable that the larger the amount of material involved in active slip, the greater is the recovery factor. But, slip will be extensive when the stress level is high. Consequently, it seems probable that the higher the stress level, the larger the recovery factor must be. The curve of recovery factor vs. stress for 75° seems to be in conformity with this hypothesis.

The influence of temperature on the recovery factor seems to be somewhat more complicated. It seems highly probable that high temperature should inhibit recovery and if this is true, then it should result in progressively decreasing recovery factors with increase of temperatures. This hypothesis seems to be borne out by the trends of the curves in Fig. 14. No explanation is offered for the negative recovery factor at this stage.

No mention has been made so far of the variation of the "instantaneous recovery factors" as a function of time in any one set of readings. In general it is found that the decay cycles in a set of readings increase first rather rapidly and then more gradually and usually end up varying in a statistical manner after a period of time. Considering a typical case such as the readings obtained at 6.696×10^6 cycles for 2000 - 75 - 1 we have them in order 568, 578, 592, 602, 611, 618, 618, 626, and 624. If these readings are divided by the first reading 568, one obtains what are defined as "instantaneous recovery factors". Since the period is also measured in these cases, these instantaneous recovery factors can be plotted as a function of time. In order to make the time also non-dimensional, the time taken for each reading is divided by that for the first reading and the first reading is plotted at the point (1, 1) in the curve. The resulting curve which is typical is shown in Fig. 15 and depicts the trends indicated above.

To conclude, one notices a certain amount of evidence in confirmation of the temporary mobility theory of slip bands in the experimental facts and analysis presented above.

d. Discussion of Trends in Damping-Fatigue Relations

Due to the paucity of test results available at this stage of testing, attempt has been made to draw only very general conclusions. Further tests are necessary in order to confirm these conclusions.

The data in this section is presented in the form of two sets of graphs. In all these, the variation of damping is represented as a

function of the number of stress reversals. In the graphs presented in Figs. 16 to 19, the curves in each figure have the same constant temperature, but each curve has its own parametric value of stress in forced vibrations. Thus, for example, in Fig. 16, all the curves are for test specimens with the same temperature of 75°F but with different parametric values of stress. In the graphs presented in Figs. 20 to 23, the curves have the same stress but with different parametric values of temperature. This set of curves are the same as those in Figs. 16 to 19 but differently grouped. In all the cases, the numbers of stress reversals are plotted on a log scale, while the value of δ is plotted on a linear scale. Since the first damping value is determined after more than 10,000 cycles, the scale starts with 10^4 . However, the value of damping for the annealed specimen just before the test is started is plotted on the y-axis and is joined by a dotted line to the first point obtained after the test has started. Consequently, the only significant item in this region is the nature of the slope but not the magnitude, which is distorted. While calculating the damping, the average value $1/n_{ave}$ is used in the expression for δ .

General trends indicated in Figs. 16 to 19:

In Fig. 16, one notices an increase of slope of the curves between $N = 0$ and $N = 10^5$ with an increase of stress. In general, the damping seems to increase rather rapidly in the beginning and then gradually decrease, sometimes to the starting value itself and at other times (higher stress levels) to a value somewhat higher than the starting value. The undulations of the curves do not indicate any trend

and seem to be quite unpredictable. This behavior is noticeable in all the other test specimens also. It is also clear from the curves presented in this figure that up to 3500 psi, the variation of damping with stress history is not appreciable.

In Fig. 17, drawn for a temperature of 225°F, the final values of damping are in general higher than the starting values. The positive slope of the damping curves in the $N = 0$ to 10^5 range is observable here also, but no trends towards increase of damping with stress is noticeable in this range. Test specimen 6000 - 225 - 1 shows a trend towards a substantial increase in damping just before it breaks at 4.618×10^6 cycles.

In the graphs presented in Fig. 18, the most significant thing one notices is the negative slope of all the curves. Thus it seems that the critical temperature of 375°F in the δ vs. T relation for an annealed specimen does also in some way affect the variation of damping with stress history. Here and there one notices an increase in damping but there is a definite general trend towards a decrease of damping with stress history except when the specimen is about to break.

In the graphs presented in Fig. 19, one again notices a general change towards a positive slope in the $N = 0$ to 10^5 range. The slightly negative value of the slope noticeable for the test specimen 3500 - 525 - 1 is not considered significant. One can also notice that those specimens which did not break at this temperature have a smaller damping in the end than at the beginning.

Thus, looking at the sets of curves presented in these four figures, the most significant thing one notices is that, whereas at all

the other temperatures at which the specimens are tested, the δ - N curves have a positive slope in the $N = 0$ to 10^5 range, those at the temperature of 375°F have a negative slope in the same range. It is also noticed that whereas the overall damping values may show either an increase or decrease, a detailed hour by hour variation of damping shows quite unpredictable variations of increase and decrease in a complex pattern after a large number of cycles of the order 10^6 .

The curves presented in Figs. 20 to 23 are a rearrangement of the previous curves in a manner described before. Unlike the previous set, the scale along the y-axis is kept constant for all these curves. The following general trends seem to be significant in this series:

At room temperature, the variation of damping is substantially of a smaller order for the stress levels 2000 and 3500 psi. At higher temperature this is not the case. The breaking points of the curves with stress level 6000 psi and different temperatures seem to fall approximately on a straight line. The corresponding line for the stress level 5000 psi has a smaller slope as compared with that for 6000 psi. This appears to be quite reasonable since in general a lower stress level means an increased fatigue life.

By the method of cross plotting of the curves presented in Figs. 20 to 23 one can obtain the variation of damping as a function of temperature after various numbers of cycles for each stress level. These curves are represented in the figures 24 to 27. The curve with the parameter "0" cycles is that obtained by plotting the damping for the annealed specimens. As it has been shown already, these "0" parameter curves have a peak at 375°F . The other curves plotted at

5×10^5 , 10^5 , 5×10^5 ; 10^6 , 5×10^6 , 10^7 , and 3×10^7 do not indicate such a peak but suggest the possibility of the peak shifting towards the right with the advent of fatigue stressing. In addition, these curves also bring out the point that except at 2000 psi, the orders of magnitude involved in damping changes are higher at 375°F than at other temperatures.

VIII. SUMMARY OF RESULTS OBTAINED

In this preliminary investigation of trends in the fatigue-damping relations, the following significant trends have been observed.

(1) Below a stress level of 112 psi in torsion, the internal friction in a 3S-O test specimen in an annealed state is not influenced by stress history. At higher stresses than this value, the damping curves of free vibration have a variable and higher slope, indicating thereby variable internal friction. Since all the other conditions that can possibly influence this result remain constant during the test, this change of damping at stress levels higher than 112 psi can be attributed to the increase in stress levels only.

(2) There exists a critical temperature of 375°F at which the internal friction of an annealed 3S-O aluminum test specimen as measured by the logarithmic-decrement method is a maximum, with lower values on either side in the tested range of temperatures up to 580°F .

(3) As further evidence towards the temporary mobility theory of slip bands, a strong tendency towards recovery in damping is noticed in the test specimens. This recovery is defined as the variation in damping of a test specimen with time, immediately after stopping a sequence of forced vibration at a stress level higher than 112 psi. In general, this recovery is found to increase with increase of stress level of forced vibrations. Its variation with temperature is somewhat more complicated. Thus, at 2000 psi, the recovery is positive at 75° and negative at 225° and 375°F with no recovery at 525°F . At higher stress levels, even at temperatures of 225° and 375°F the recovery is positive

and goes to no recovery at 525°F.

(4) At room temperature, the variation of damping with stress for an annealed specimen shows a strong tendency towards an increase in damping with stress in the first few thousand cycles of forced vibrations.

(5) At and below 3500 psi and 75°F, the damping which slightly increases in the beginning, goes down to almost the starting value after a complex pattern of increase and decrease within small limits. This complex pattern of increase and decrease of damping within small limits was observable at higher temperatures also in all the specimens which did not break within 30×10^6 cycles up to which the specimens were tested.

(6) At 5000 psi and 6000 psi the damping variations are far more pronounced than at the lower stress levels.

(7) There is a tendency for the extrapolated points of failure on the δ - N curves for the same stress level but at various temperatures to fall approximately on a straight line. In addition the slope of this straight line which could be drawn for the stress levels of 5000 psi and 6000 psi decreases with decrease of stress, thus predicting a higher fatigue life at lower stress levels and temperatures.

(8) The slope of the δ vs. N curve in the $N = 0$ to 10^5 range is positive in all cases except at the temperature 375°F. At this temperature, however, the slope is negative indicating a reduction in damping with the stress history as compared to the annealed value.

(9) At this stage of testing, the critical temperature of 375°F does not show any significant bearing on the fatigue life of the specimens as it has been originally suggested.

(10) The δ vs. T relation during the progress of stress history at various stress levels suggests the possibility of the critical temperature increasing with stress history. In addition, it is found that except at 2000 psi, the orders of magnitude involved in changes of damping are higher at 375°F than at other temperature.

IX. A CRITICISM OF TECHNIQUES AND RECOMMENDATIONS

It is not out of place here to discuss briefly the validity of some of the methods adopted in analyzing the results obtained in the above series of tests. While it is freely recognized that experimental scatter is inherent in all fatigue testing, the question always arises "What amount of the observed scatter is due to the experimental techniques and how much can be attributed to the material itself." This is a moot question to answer in experimental research and is more so in problems of fatigue. It is believed that in this work definite efforts have been made to reduce the errors involved in measurements and the variations observed are mostly inherent and not due to extraneous factors.

However, one notices in the recovery phenomena a substantial amount of scatter in some cases. In the absence of any trend in the variation of the recovery factors with the number of reversals of stress, it does not seem probable that such large scatter should exist even in a few cases. It is therefore felt that much further work is necessary in this direction in order to investigate this problem of scatter.

It will also be noticed that while plotting the fatigue-damping relations, the average of the six "decay cycle" readings is taken to represent the damping at any instant. This is clearly arbitrary. This becomes all the more significant in the presence of the phenomena of "recovery". A justifying reason that can be offered is, that in most of the cases a tendency towards the "decay cycles" to vary in a random manner after approximately six to eight readings has been observed.

The possibility of measuring damping immediately after stopping the forced vibration and taking it as a measure of damping is very tempting but it is found extremely difficult to control the short period of elapsed time between stopping the forced vibrations and measuring the damping. On the other hand, the idea of measuring the damping after a period of rest after forced vibration is not appealing either, since in this case one largely neglects the effect of recovery. It consequently seems that some further work is necessary in order to determine what value of damping of the specimen is most desirably measured in order that it may represent the true state of affairs in the fatigue-damping relations. In the absence of prior work in this field at this stage, it is considered desirable to take the average of the six "decay cycle" readings while determining the damping at any instant. In order to indicate the amount of scatter and recovery involved, the curves in Fig. 16 are reproduced in Fig. 28 with the scatter band points also included. The points plotted correspond to maximum, arithmetical mean and minimum of the internal friction at any instant.

Similar comments also seem to be pertinent in connection with the possibilities of predicting fatigue life at various temperatures. A sufficient number of tests should be conducted in order that one may determine the scatter bands involved in this problem. It would be too much to expect that they would yield straight line relations. It is suggested that stress levels of 4000, 5500, and 6500 psi are worth investigating to determine the validity of this suggestion.

Cross plotting of δ vs. T for each stress level at various stages of stress history seem to suggest the possibility of the critical

temperature shifting towards the right (increasing). It is consequently suggested that higher testing temperatures, preferably at least 675°F, may be profitably investigated.

The effect of large periods of rest on damping in fatigue stressing has not been investigated in this work. There are some indications that a larger recovery than is noticed in the above work may be possible. It is therefore suggested that the influence of periods of rest of the order of 2 to 12 hours on both fatigue and damping at room and higher temperatures be investigated.

Because of the high frequencies used, it has not been possible to observe the variation of damping in the first 50,000 cycles of fatigue stressing. It is considered desirable to investigate the fatigue-damping relations in this range of stress history.

REFERENCES

1. H. J. Gough, "Crystalline Structure in Relation to Failure of Metals, Especially by Fatigue", Edgar Marburg Lecture, ASTM, Vol. 33, Part II, 1933.
2. C. S. Barrett, "Structure of Metals", McGraw-Hill Book Co., 1943.
3. G. I. Taylor and C. F. Elam, "The distortion of an Aluminum Crystal During a Tensile Test", Roy. Soc. London Proc., A, Vol. 102, 1923.
4. E. Orowan, "Zeit. Physik", Vol. 89, p. 634, 1934.
5. M. Polanyi, "Zeit. Physik", Vol. 89, p. 660, 1934.
6. G. I. Taylor, "Roy. Soc. London Proc.", A, Vol. 145, p. 362, 1934.
7. C. Zener, "Elasticity and Anelasticity", University of Chicago Press, 1948.
8. D. Hanson and M. A. Wheeler, "J. Inst. of Metals", Vol. 45, p. 229, 1931.
9. H. C. H. Carpenter, "J. Iron Steel Inst.", Vol. 107, p. 175, 1923.
10. T. S. Kê, "Experimental Evidence of the Viscous Behavior of Grain Boundaries in Metals", Phys. Rev., LXXI (1943), p. 533.
11. W. Rosenhain, "Deformation and Fracture in Iron and Steel", J. Iron and Steel Inst., LXX (1906), p. 189.
12. W. Rosenhain, "Introduction to Physical Metallurgy", Constable and Company, 1919.
13. "Report on a Conference in Internal Strains in Solids", Roy. Soc. London Proc., Vol. 52, p. 1, 1940.
14. Lord Kelvin, "Math. and Physical Papers", Vol. III, p. 23.
15. B. J. Lazan, "A Study with New Equipment of the Effects of Fatigue Stress on Damping Capacity and Elasticity of Mild Steel", ASTM Trans., Vol. 4, p. 499, 1950.
16. B. J. Lazan and T. Wu, "Damping, Fatigue and Dynamic Stress Strain Properties of Mild Steel", ASTM Proc., Vol. 51, 1951.

17. B. J. Lazan and L. J. Demer, "Damping Elasticity and Fatigue Properties of Temperature-Resistant Materials", WADC TR 52-243.
18. L. J. Demer and B. J. Lazan, "Damping, Elasticity and Fatigue Properties of Unnotched and Notched N-133 at Room and Elevated Temperatures", WADC Report 53-70.
19. L. J. Demer and B. J. Lazan, "The Effect of Stress Magnitude, and Stress History on the Damping, Elasticity and Fatigue Properties of Metallic Materials", Dept. of Mechanics and Materials, University of Minnesota.
20. A. M. Freudenthal, "The Inelastic Behavior of Engineering Materials and Structures", John Wiley & Sons, Inc., 1950.
21. W. H. Wittrick, "The Properties of Crossed Flexure Pivots and the Influence of the Points at Which the Strips Cross", The Aeronautical Quarterly, RAS, Vol. 2, February 1951.
22. E. Epremian and R. F. Mehl, "Investigation of the Statistical Nature of Fatigue Properties", NACA TN 2719.
23. G. E. Dieter and R. F. Mehl, "Investigation of the Statistical Nature of Fatigue of Metals", NACA TN 3019.
24. P. J. E. Forsyth, "Some Further Observations on the Fatigue Process of Aluminum", RAE Report No. Met. 70, December 1952.

Table 1

2000-75-1

No. of Reversals	n ₁	n ₂	n ₃	n ₄	n ₅	n ₆	Ave n	1/n x 10 ³	Max ^m diff.	Significant Recovery Factor
0	669	651	649	649	652	651	654	1.53	20	
46500	451	457	478	485	492	520	481	2.08	69	1.15
93000	412	416	420	422	426	428	421	2.38	16	1
186000	444	429	414	405	425	425	424	2.36	39	.96
279000	461	462	435	430	428	412	438	2.28	49	.90
558000	559	550	550	563	553	560	556	1.80	13	1
837000	474	503	521	521	523	530	512	1.96	56	1.12
2.511x10 ⁶	496	507	525	536	552	555	527	1.90	59	1.12
3.348x10 ⁶	571	569	573	568	573	575	572	1.75	7	1
6.696x10 ⁶	568	578	592	602	611	618	595	1.68	50	1.09
10x10 ⁶	584	585	593	589	597	599	593	1.68	15	1
13.39x10 ⁶	608	608	609	619	629	634	618	1.62	26	1.04
16.92x10 ⁶	586	583	598	608	621	633	607	1.65	50	1.09
23.43x10 ⁶	624	618	634	643	645	634	633	1.58	27	1.04
26.78x10 ⁶	639	642	667	674	682	702	668	1.50	63	1.10
30.13x10 ⁶	640	646	660	670	670	678	661	1.51	38	1.08

Specimen did not break

Table 2
2000-225-1

No. of Reversals	n ₁	n ₂	n ₃	n ₄	n ₅	n ₆	n _{ave}	1/nave x 10 ³	Max ^m diff.	Significant Recovery Factor
0	182	182	184	182	181	181	182	5.5	3	
46500	149	150	150	150	151	150	150	6.65	2	1.00
93000	142	143	142	144	144	147	144	6.90	5	1.04
186000	150	148	145	147	147	149	148	6.75	5	.99
279000	148	151	147	146	142	145	147	6.8	9	.98
558000	157	156	157	156	154	153	156	6.4	4	.97
837000	151	146	147	143	137	136	143	7	15	.90
1.65x10 ⁶	179	179	180	180	178	176	179	5.58	4	.98
3.35x10 ⁶	190	184	182	182	181	179	183	5.46	11	.94
6.696x10 ⁶	195	187	185	185	185	185	187	5.32	10	.96
10x10 ⁶	196	193	191	189	186	199	192	5.2	10	.95
14.22x10 ⁶	187	178	176	174	175	174	177	5.65	13	.93
16.92x10 ⁶	192	185	181	180	176	175	182	5.5	17	.91
23.4x10 ⁶	186	182	183	182	183	183	183	5.46	4	.98
26.78x10 ⁶	170	174	165	159	157	155	163	6.14	15	.91
30.13x10 ⁶	172	170	169	165	164	164	168	5.95	8	.95

Specimen did not break

Table 3
2000-375-1

No. of Reversals	n ₁	n ₂	n ₃	n ₄	n ₅	n ₆	n _{ave}	1/n _{ave} × 10 ³	Max ^m Diff.	Significant Recovery Factor
0	35	35	35	35	35	35	35	28.6	0	
46000	40	40	40	40	40	39	40	25.0	1	1
93000	43	43	45	41	45	47	44	22.7	6	1.09
186000	43	44	43	44	43	42	43	23.3	2	1
279000	41	42	42	42	41	41	42	23.8	1	1
558000	47	47	47	47	47	47	47	21.3	0	1
837000	52	52	51	51	50	49	51	19.6	3	.94
1.1 × 10 ⁶	53	52	51	51	51	50	51	19.6	3	.94
1.65 × 10 ⁶	52	50	50	51	50	50	51	19.6	2	.96
3.35 × 10 ⁶	54	54	52	52	52	52	53	18.85	2	.96
6.69 × 10 ⁶	57	57	57	55	55	55	56	17.85	2	.96
10 × 10 ⁶	62	61	60	59	59	59	60	16.68	3	.95
13.22 × 10 ⁶	62	60	58	58	57	56	59	16.95	6	.90
16.92 × 10 ⁶	59	57	56	56	50	55	57	17.55	4	.93
23.44 × 10 ⁶	56	57	56	56	50	55	56	17.85	2	.98
26.78 × 10 ⁶	61	57	56	55	50	55	57	17.55	6	.90
30.13 × 10 ⁶	60	57	56	55	50	55	56	17.85	5	.92

Specimen did not break

Table 4
2000-525-1

No. of Reversals	n ₁	n ₂	n ₃	n ₄	n ₅	n ₆	n _{ave}	1/n _{ave} x 10 ³	Max ^m diff.	Significant Recovery Factor
0	38	36	35	36	35	37	36	27.8	3	
46500	31	32	31	31	30	31	31	32.3	2	1
93000	30	31	31	31	30	30	31	32.3	1	1
186000	33	35	33	33	33	33	33	30.3	2	1
279000	33	33	34	33	33	33	33	30.3	1	1
558000	36	36	35	35	36	35	36	27.8	1	1
837000	37	38	39	37	37	37	38	26.3	2	1
1.65x10 ⁶	42	40	40	39	44	39	41	24.4	3	1
3.35x10 ⁶	42	45	43	41	42	41	42	23.8	4	1
6.696x10 ⁶	43	45	43	49	45	45	44	22.7	2	1
10x10 ⁶	46	51	46	43	43	45	46	21.7	8	1
13.39x10 ⁶	49	47	46	46	46	48	47	21.3	3	1
16.74x10 ⁶	47	51	47	47	46	47	48	20.8	5	1
23.46x10 ⁶	48	48	48	50	50	49	49	20.4	2	1
27x10 ⁶	46	48	48	50	50	50	49	20.4	4	1
28.61x10 ⁶	49	49	51	48	46	46	49	20.4	5	1

Specimen did not break

Table 5
3500-75-1

No. of Reversals	n ₁	n ₂	n ₃	n ₄	n ₅	n ₆	n _{ave}	1/nave x 10 ³	Max ^m diff.	Significant Recovery Factor
0	655	653	620	627	632	651	639	1.57	35	
46500	433	445	453	469	434	479	452	2.21	46	1.10
93000	468	509	496	522	529	534	509	1.97	66	1.14
186000	476	472	470	473	474	479	474	2.15	9	1
279000	445	470	503	501	523	526	495	2.02	81	1.82
558000	468	486	488	511	511	513	496	2.02	45	1.10
837000	503	511	519	538	544	522	523	1.91	41	1.08
1.674x10 ⁶	418	455	480	482	497	495	471	2.12	77	1.18
3.35x10 ⁶	460	496	508	507	517	522	502	2.00	62	1.14
6.69x10 ⁶	412	445	465	486	456	465	455	2.2	74	1.17
10x10 ⁶	417	455	473	486	495	501	471	2.12	84	1.2
14.5x10 ⁶	452	458	477	488	505	510	482	2.08	62	1.13
16.75x10 ⁶	466	493	504	522	528	533	508	1.97	67	1.15
23.44x10 ⁶	464	492	505	512	521	525	503	1.99	61	1.14
26.78x10 ⁶	488	496	513	520	525	530	512	1.96	42	1.09
30.13x10 ⁶	485	505	495	515	520	525	508	1.97	40	1.09

Specimen did not break

Table 6

3500-225-1

No. of Reversals	n ₁	n ₂	n ₃	n ₄	n ₅	n ₆	n _{ave}	1/nave x 10 ³	Max ^m _{diff.}	Significant Recovery Factor
0	175	176	186	177	197	194	184	5.45	22	
46500	184	180	168	196	195	194	186	5.45	28	1
93000	180	179	172	181	176	179	178	5.62	9	1
186000	180	169	166	176	185	181	176	5.67	19	1
279000	170	164	163	168	164	165	166	6.02	7	1
558000	168	173	175	181	184	180	177	5.65	16	1
837000	186	184	196	175	181	180	184	5.45	21	1
1.65x10 ⁶	172	182	194	178	178	177	180	5.55	22	1
3.35x10 ⁶	171	164	190	173	180	179	173	5.78	16	1
6.69x10 ⁶	169	174	174	175	180	180	175	5.71	11	1
10x10 ⁶	163	168	165	169	165	165	166	6.02	6	1
13.39x10 ⁶	137	142	143	147	144	144	143	6.98	10	1
16.92x10 ⁶	135	140	138	142	144	144	140	7.14	9	1
23.44x10 ⁶	132	139	139	138	142	140	138	7.25	10	1
26.78x10 ⁶	136	140	136	136	135	135	136	7.35	5	1
30.13x10 ⁶	133	136	135	133	134	134	134	7.46	5	1

Specimen did not break

Table 7
3500-375-1

No. of Reversals	n ₁	n ₂	n ₃	n ₄	n ₅	n ₆	n _{ave}	1/n _{ave} x 10 ³	Max ^m diff.	Significant Recovery Factor
0	36	38	40	38	40	40	39	25.6	4	
52500	53	55	52	50	51	51	52	19.2	5	1.00
105000	55	57	57	57	64	57	58	17.25	9	1.00
210000	62	65	64	69	69	70	67	14.95	8	1.13
315000	58	63	62	69	62	62	63	16.15	11	1.00
630000	62	62	60	61	66	63	63	16.15	3	1.00
945000	62	63	63	61	63	64	63	16.15	2	1.00
1.89x10 ⁶	66	64	70	69	67	71	70	14.3	4	1.00
3.78x10 ⁶	73	84	81	80	80	87	81	12.35	14	1.00
7.56x10 ⁶	75	75	77	73	81	75	76	13.3	8	1.00
11.34x10 ⁶	75	83	75	84	86	76	80	12.5	11	1.00
15.12x10 ⁶	75	80	75	85	72	72	77	13.0	13	1.00
18.9x10 ⁶	71	75	73	77	72	80	74	13.5	9	1.13
26.54x10 ⁶	80	90	74	81	73	71	78	12.85	19	1.00
30.2x10 ⁶	80	76	75	76	76	76	78	12.85	5	1.00

Specimen did not break

Table 8
3500-525-1

No. of Reversals	n ₁	n ₂	n ₃	n ₄	n ₅	n ₆	n _{ave}	l _{nave} x 10 ³	Max ^m diff.	Significant Recovery Factor
0	50	52	51	52	51	52	51	19.6	2	
52500	55	54	53	53	54	54	54	18.5	1	1
105000	51	52	48	53	50	51	51	19.6	7	1
210000	47	49	48	47	47	48	48	20.8	2	1
315000	48	50	48	48	52	48	49	20.4	4	1
630000	44	45	44	44	46	44	45	22.2	2	1
945000	50	50	50	54	50	48	50	20.0	6	1
1.89x10 ⁶	47	47	46	45	43	48	46	21.7	5	1
3.78x10 ⁶	49	47	45	46	48	49	47	21.3	4	1
7.56x10 ⁶	56	52	53	60	53	54	55	18.2	8	1
11.34x10 ⁶	46	52	50	50	49	49	49	20.4	6	1
15.12x10 ⁶	52	50	48	48	53	53	51	19.6	5	1
18.9x10 ⁶	48	53	48	47	47	47	48	20.8	6	1
26.46x10 ⁶	50	52	52	52	48	52	51	19.6	4	1
30.24x10 ⁶	51	51	51	51	55	49	51	19.6	6	1

Specimen did not break

Table 9

5000-75-1

No. of Reversals	n ₁	n ₂	n ₃	n ₄	n ₅	n ₆	n _{ave}	l _{/nave} x 10 ³	Max ^m diff.	Significant Recovery Factor
0	811	803	828	801	808	809	810	1.24	27	
52500	253	274	285	296	293	298	283	3.53	45	1.18
105000	249	264	276	296	302	310	283	3.53	61	1.25
210000	301	316	320	320	321	329	318	3.14	28	1.09
315000	291	294	298	300	303	298	297	3.37	12	1
630000	275	316	335	331	314	355	321	3.11	80	1.29
945000	291	323	314	321	323	328	311	3.2	37	1.13
1.89x10 ⁶	336	343	369	397	384	392	370	2.7	61	1.16
3.78x10 ⁶	413	400	367	364	377	397	386	2.59	49	.96
7.56x10 ⁶	356	374	367	358	364	365	364	2.75	18	1
11.34x10 ⁶	381	368	377	366	395	385	379	2.64	29	1.04
15.44x10 ⁶	377	364	386	388	410	415	390	2.56	51	1.1
18.9x10 ⁶	345	351	365	409	422	414	384	2.61	77	1.2
26.57x10 ⁶	397	430	435	431	430	428	425	2.35	38	1.08
30.20x10 ⁶	368	372	390	400	413	430	396	2.53	62	1.13

Specimen did not break

Table 10

5000-225-1

No. of Reversals	n ₁	n ₂	n ₃	n ₄	n ₅	n ₆	n _{ave}	$l_{nave} \times 10^3$	Max ^m Diff.	Significant Recovery Factor
0	215	212	215	215	212	216	214	4.67	4	
52500	133	138	146	144	147	142	142	7.05	13	1.07
105000	158	166	168	170	172	172	168	5.95	14	1.09
210000	166	169	173	174	175	180	173	5.75	14	1.08
315000	146	141	146	150	151	155	148	6.75	14	1.06
630000	155	160	167	169	171	173	166	6.02	18	1.12
945000	152	149	157	157	158	162	156	6.4	13	1.07
1.89×10^6	170	169	176	181	184	185	178	5.62	16	1.09
3.78×10^6	163	165	168	178	179	179	172	5.82	16	1.10
7.56×10^6	160	162	167	171	173	170	167	5.98	13	1.06
11.34×10^6	160	161	157	157	162	168	161	6.2	11	1.05
15.12×10^6	172	170	165	170	171	172	170	5.88	7	1
18.9×10^6	168	167	175	176	181	182	175	5.71	15	1.08
26.4×10^6	165	169	171	174	177	178	172	5.82	13	1.08
30.2×10^6	158	164	164	168	171	171	166	6.02	14	1.08

Specimen did not break

Table 11

5000-375-1

No. of Reversals	n ₁	n ₂	n ₃	n ₄	n ₅	n ₆	n _{ave}	$\frac{1}{n_{ave}} \times 10^3$	Max ^m diff.	Significant Recovery Factor
0	36	35	34	34	33	35	35	28.6	3	
52500	43	45	43	47	45	46	45	22.2	4	1
105000	49	44	50	47	47	47	47	21.3	6	1
210000	48	46	47	48	49	51	48	20.8	5	1
315000	54	54	50	54	54	48	54	18.5	6	1
630000	58	59	58	55	57	56	57	17.5	4	1
945000	60	59	57	59	58	58	59	16.95	3	1
1.89×10^6	61	58	69	72	58	56	62	16.12	16	1
3.78×10^6	64	61	66	68	63	68	65	15.4	7	1
7.56×10^6	63	56	59	62	60	64	61	16.4	8	1
11.34×10^6	65	64	61	63	61	63	63	15.9	4	1
15.168×10^6	Specimen broke.						Extrapolated Value.			
								15.8		

Table 12
5000-525-1

No. of Reversals	n ₁	n ₂	n ₃	n ₄	n ₅	n ₆	n _{ave}	1/n _{ave} x 10 ³	Max ^m diff.	Significant Recovery Factor
0	41	47	45	50	42	38	44	22.7	12	1
52500	42	39	38	40	39	39	39	25.6	3	1
105000	41	41	39	41	39	37	40	25.0	4	1
210000	37	36	41	39	39	39	39	25.6	5	1
315000	35	39	41	41	38	42	39	25.6	7	1
630000	39	38	41	38	38	39	39	25.6	3	1
945000	40	44	40	41	41	39	41	24.4	2	1
1.89x10 ⁶	41	42	41	45	41	40	42	23.8	5	1
3.78x10 ⁶	44	43	47	43	45	43	44	22.7	4	1
7.56x10 ⁶	Specimen broke.						Extrapolated Value			
								21.6		

Table 13

6000-75-1

No. of Reversals	n ₁	n ₂	n ₃	n ₄	n ₅	n ₆	n _{ave}	1/n _{ave} ³	Max ^m diff.	Significant Recovery Factor
0	762	740	767	740	760	767	756	1.47	27	
52500	220	227	251	245	240	248	239	4.17	31	1.14
105000	205	219	229	231	228	239	225	4.45	34	1.17
210000	247	263	260	250	245	260	254	3.94	16	1.00
315000	243	250	241	225	208	190	243	4.1	53	.78
630000	238	246	284	270	269	268	263	3.8	46	1.13
945000	327	334	335	321	337	367	337	2.95	40	1.12
1.89x10 ⁶	300	313	348	362	366	375	344	2.81	75	1.25
3.78x10 ⁶	341	366	370	375	396	386	372	2.69	55	1.13
5.67x10 ⁶	351	384	385	392	396	400	385	2.60	49	1.14
7.56x10 ⁶	370	383	400	402	399	398	392	2.55	32	1.00
9.45x10 ⁶	369	393	404	429	429	430	409	2.45	61	1.17
9.66x10 ⁶	Specimen broke.					Extrapolated Value.	2.45			

Table 14

6000-225-1

No. of Reversals	n ₁	n ₂	n ₃	n ₄	n ₅	n ₆	n _{ave}	$l_{\text{ave}} \times 10^3$	Max ^m diff.	Significant Recovery Factor
0	190	188	187	191	186	191	189	5.29	5	
52500	128	132	136	134	133	133	133	7.5	8	1.06
105000	155	153	153	156	150	155	154	6.5	3	1
210000	109	110	110	125	129	131	119	8.4	22	1.2
315000	128	125	125	129	128	126	127	7.87	4	1
630000	145	138	138	140	134	134	138	7.25	11	.93
945000	100	109	120	129	126	121	117	8.55	21	1.25
1.89x10 ⁶	94	105	113	120	120	121	112	8.92	27	1.29
3.78x10 ⁶	71	71	73	72	74	77	73	13.7	5	1.09
4.62x10 ⁶										
		Specimen broke.					Extrapolated Value	15.5		

Table 15
6000-375-1

No. of Reversals	n ₁	n ₂	n ₃	n ₄	n ₅	n ₆	n _{ave}	1/n _{ave} x 10 ³	Max ^m diff.	Significant Recovery Factor
0	38	38	36	38	38	36	37	27	2	
52500	47	49	47	51	48	50	49	20.4	4	1
105000	49	49	51	53	53	53	51	19.6	4	1.08
210000	48	48	48	50	48	51	49	20.4	3	1
315000	53	56	56	56	56	53	55	18.2	3	1
630000	56	57	61	61	61	56	59	16.95	5	1
945000	61	62	56	59	59	55	59	16.95	6	1
1.89x10 ⁶	62	58	63	60	63	60	61	16.4	5	1
3.78x10 ⁶	54	56	54	56	56	53	55	18.2	3	1
4.13x10 ⁶	Specimen broke.						Extrapolated Value		18.5	

Table 16

6000-525-1

No. of Reversals	n ₁	n ₂	n ₃	n ₄	n ₅	n ₆	n _{ave}	1/n _{ave} x 10 ³	Max ^m diff.	Significant Recovery Factor
0	48	48	47	47	48	50	48	20.8	3	
52500	46	46	46	47	47	48	47	21.3	2	1
105000	48	50	50	50	52	46	49	20.4	6	1
210000	49	50	49	52	49	52	50	20.0	3	1
315000	46	49	49	47	47	48	48	20.8	3	1
630000	46	45	46	48	47	48	47	21.3	3	1
945000	48	49	49	49	49	50	49	20.4	2	1
1.89x10 ⁶	46	46	46	46	48	46	46	21.7	2	1
3.465x10 ⁶	Specimen broke.						Extrapolated Value		23.25	

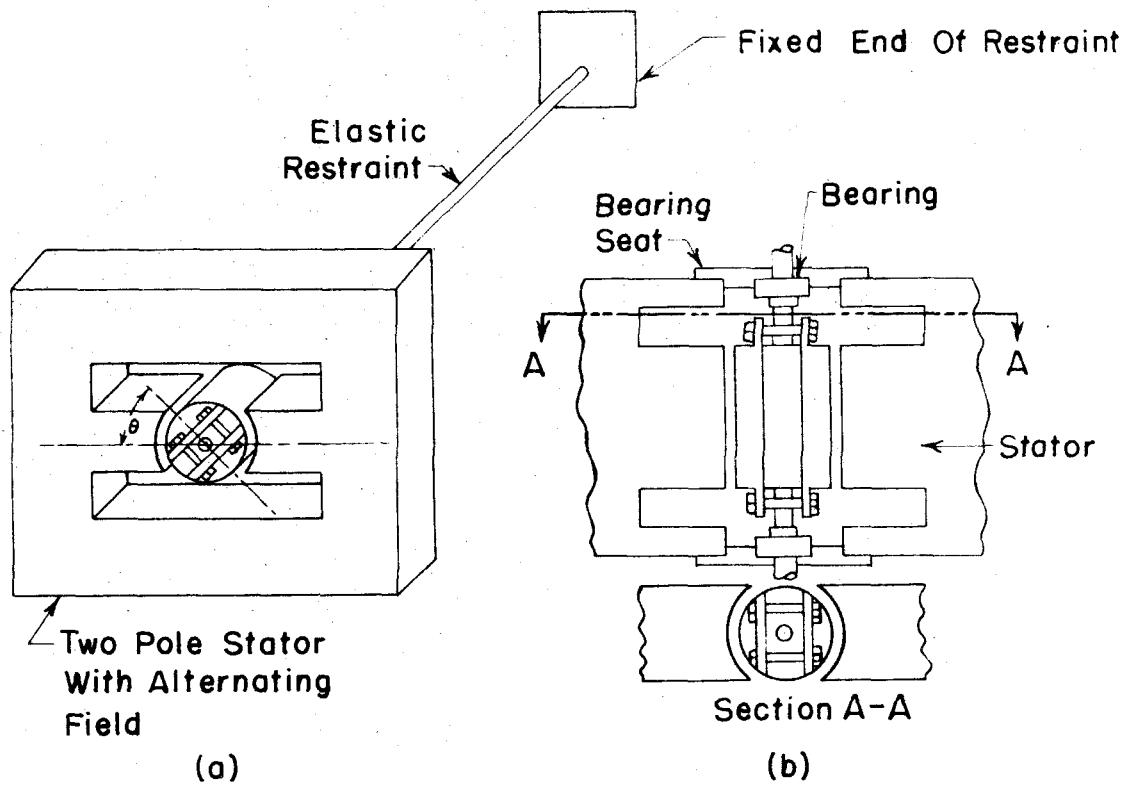


FIG. 1- SCHEMATIC DIAGRAM OF VIBRATOR

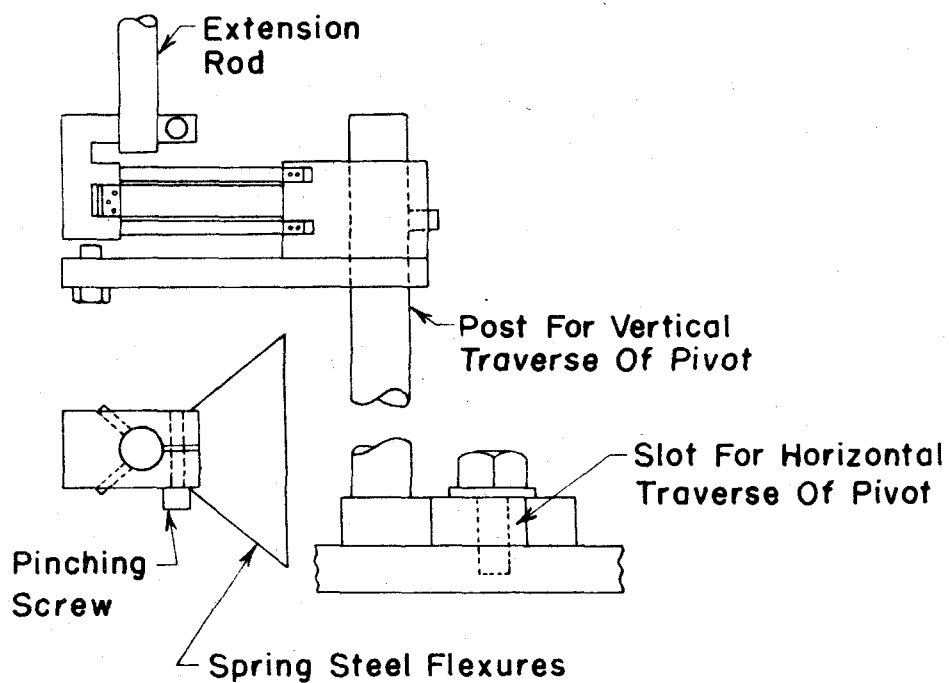


FIG. 2a-DETAILS OF FLEXURE PIVOT

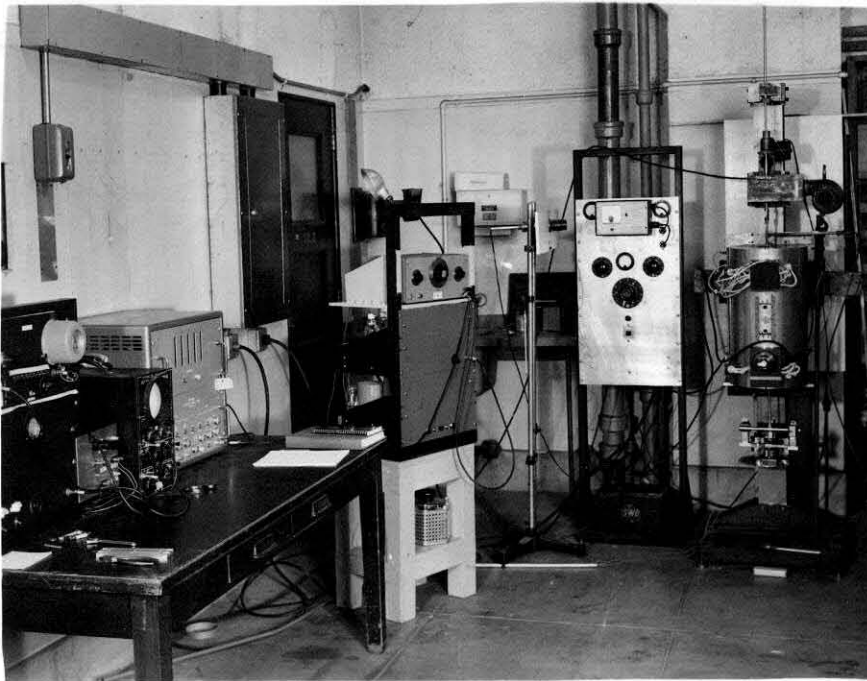


Fig. 3
General View of the Test Equipment

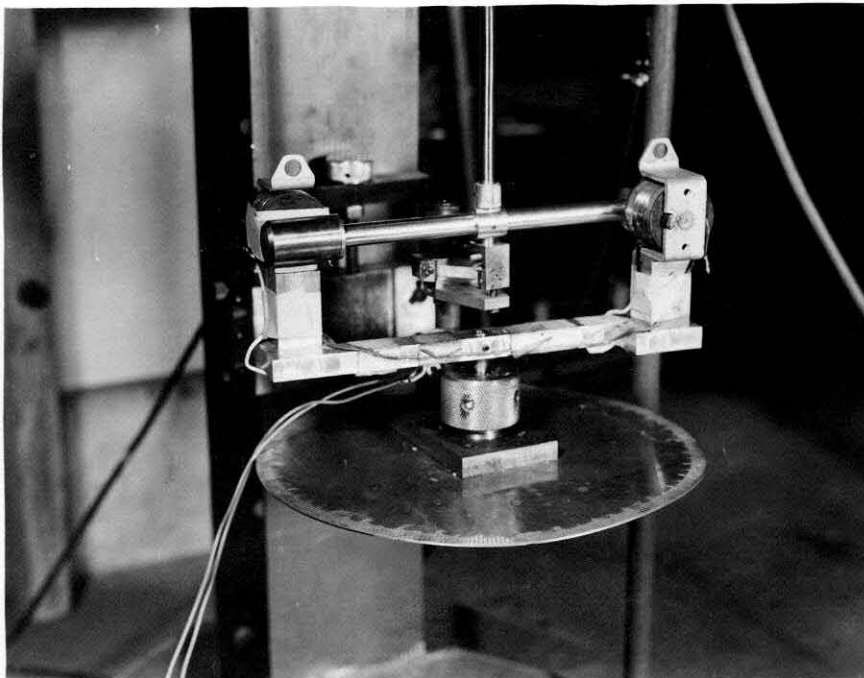


Fig. 2 B
Closeup of the Inertia Bar and Details of
Flexure Pivot

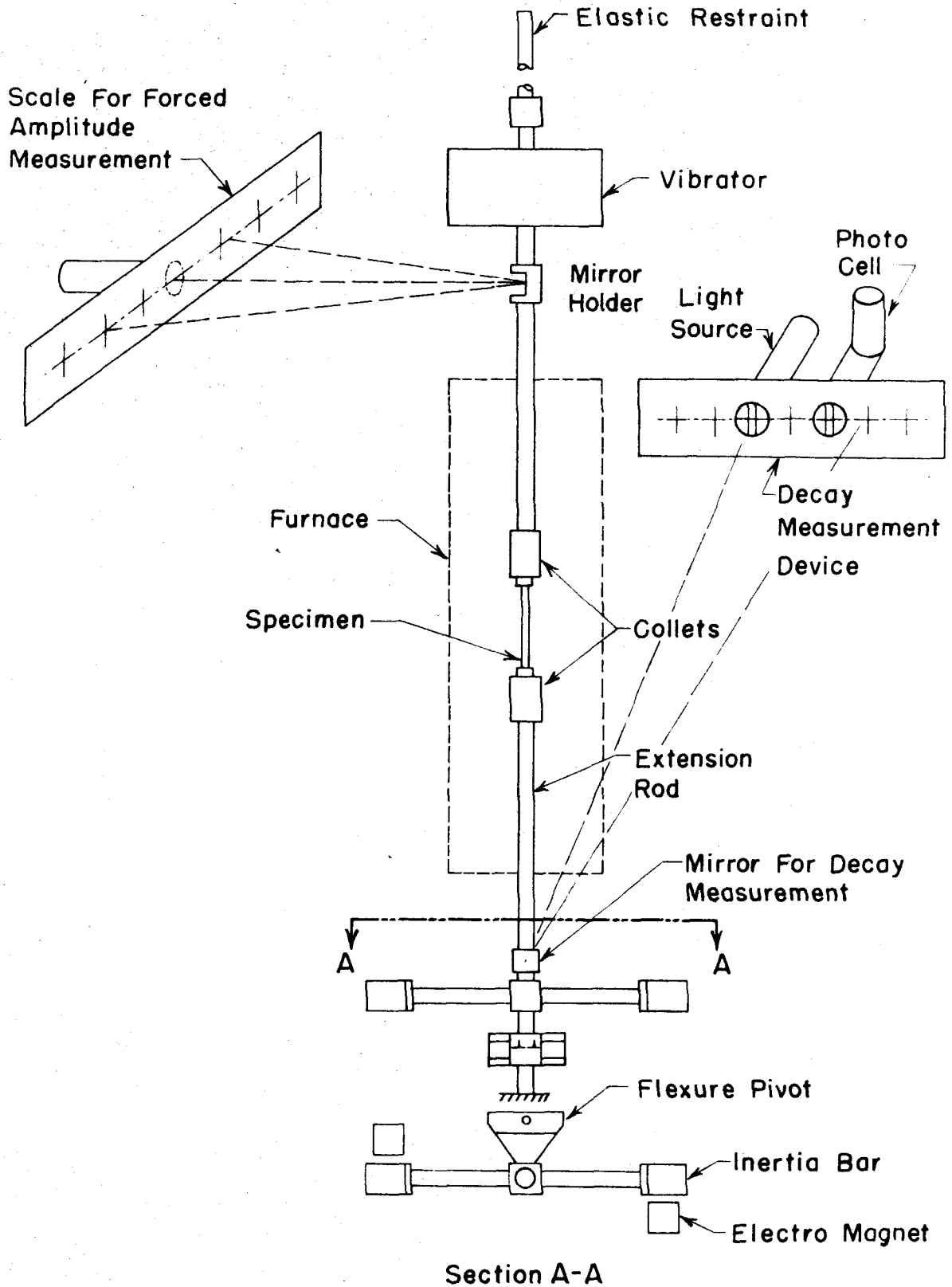


FIG.4 - SCHEMATIC DIAGRAM OF TEST SET-UP

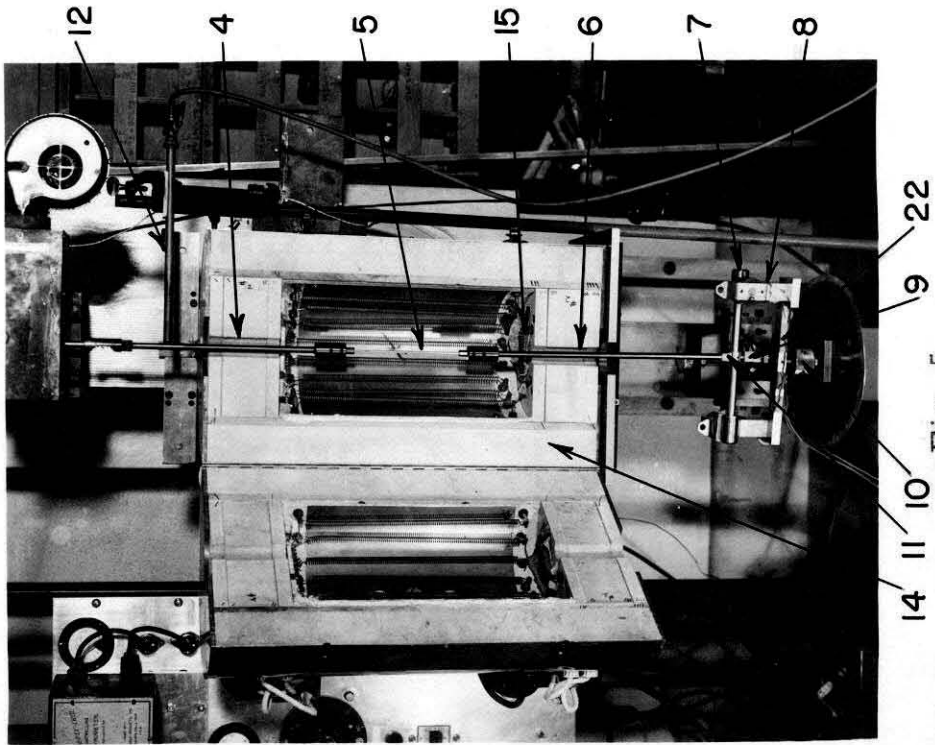


Fig. 5
Closeup of the Vibrator with the
Test Specimen Mounted

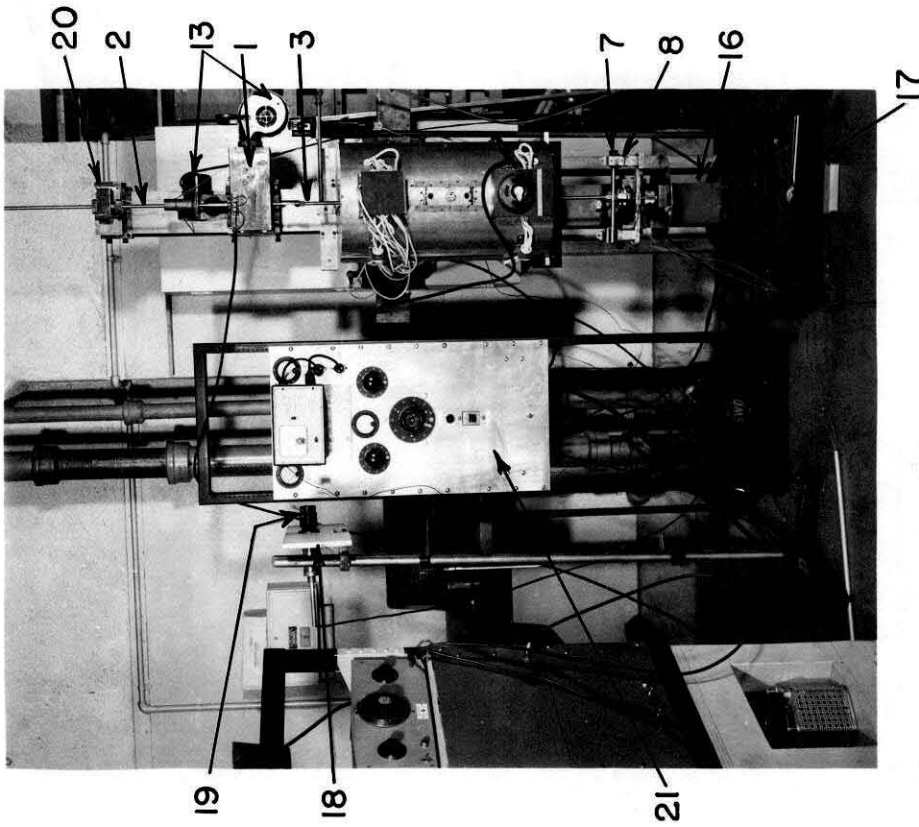


Fig. 6
General View of the Vibrator
With its Accessory Equipment

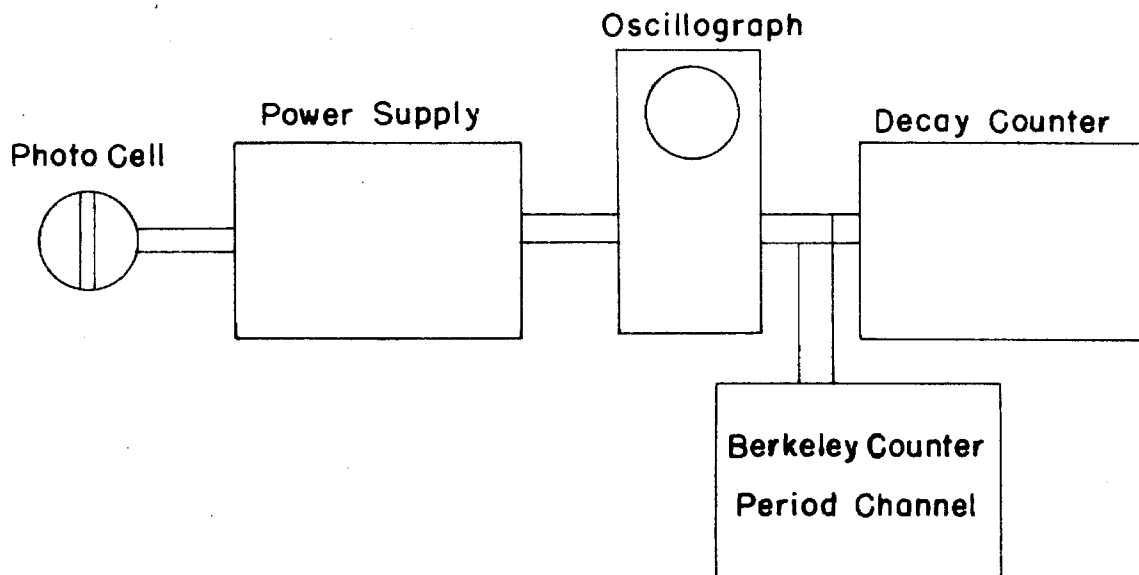


FIG.7-BLOCK DIAGRAM FOR MEASURING CIRCUIT

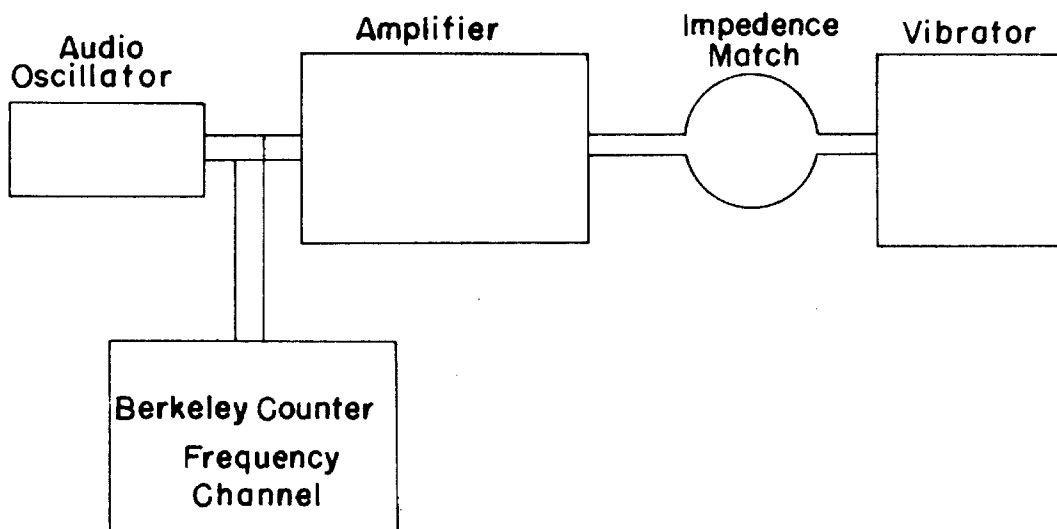
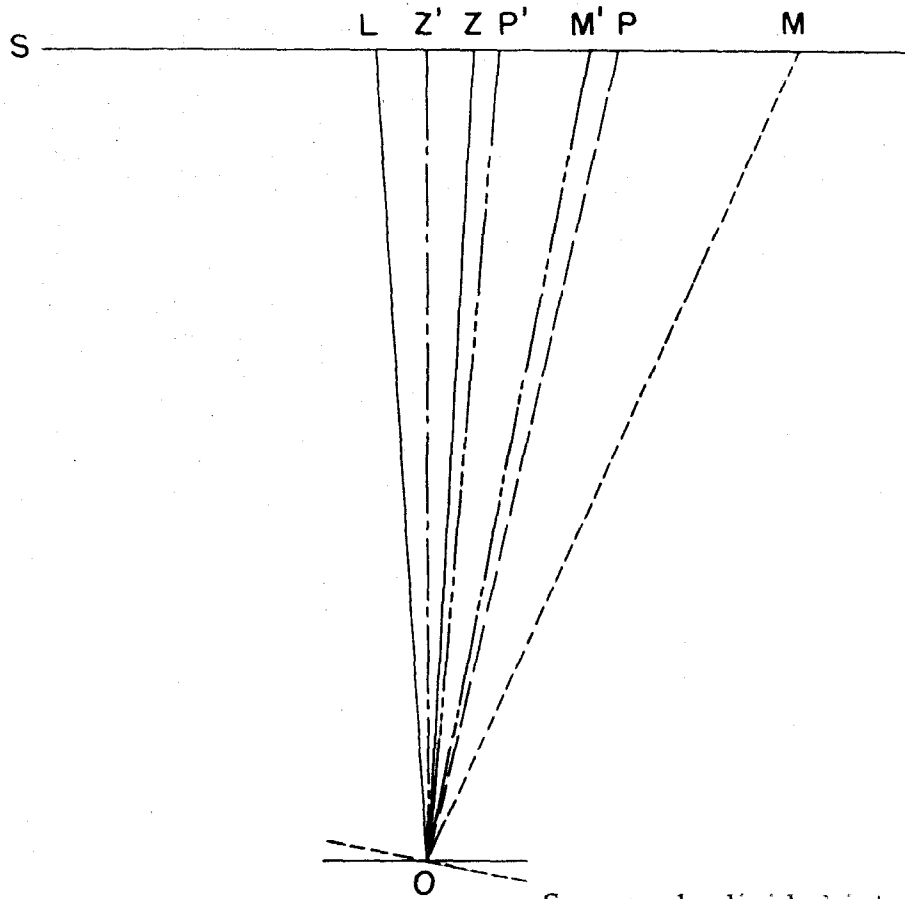


FIG.8 - BLOCK DIAGRAM FOR POWER SUPPLY TO THE VIBRATOR



$$\delta = \frac{1}{n} [\text{Log } M' \hat{O} Z' - \text{Log } P' \hat{O} Z']$$

$$= \frac{1}{n} [\text{Log } MZ - \text{Log } PZ]$$

- S scale divided into 1/20 inch
- LO incident ray
- ZO reflected ray with inertia bar in zero position
- Z'O bisector of angle LOZ
- MO reflected ray with inertia bar attracted by magnets
- M'O bisector of angle MOZ
- P location of the photo-cell slit
- P'O bisector of the angle POL

FIG. 9 - PRINCIPLE OF DECAY MEASUREMENTS

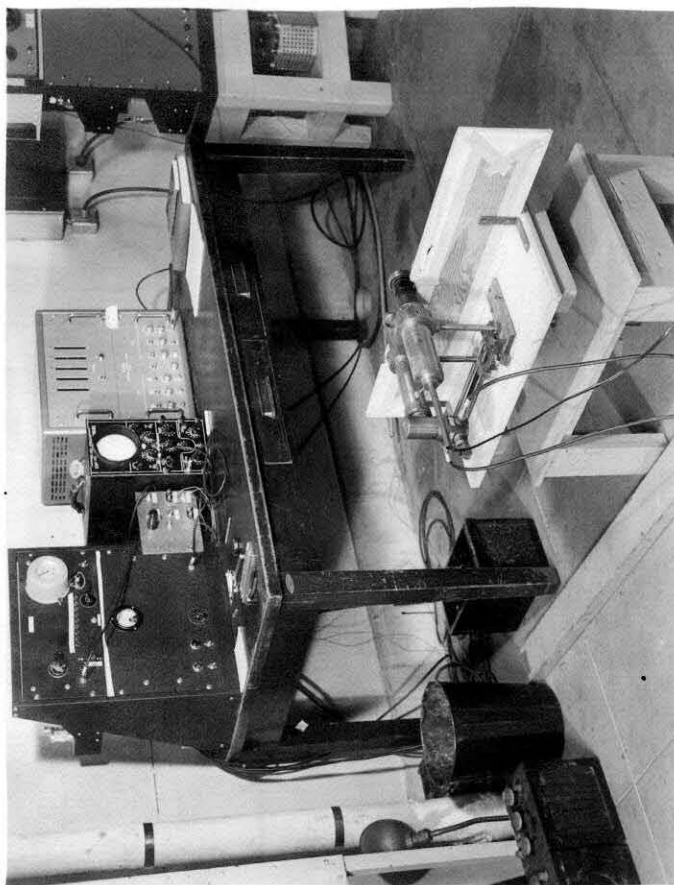


Fig. 10

Decay Measuring Equipment

On the table from left to right - power supply and electronic counter, control panel for decay measurements, monitoring oscillograph, and Berkeley Universal counter.

At the bottom on the floor is the photo-cell and light source on the adjustable stand.

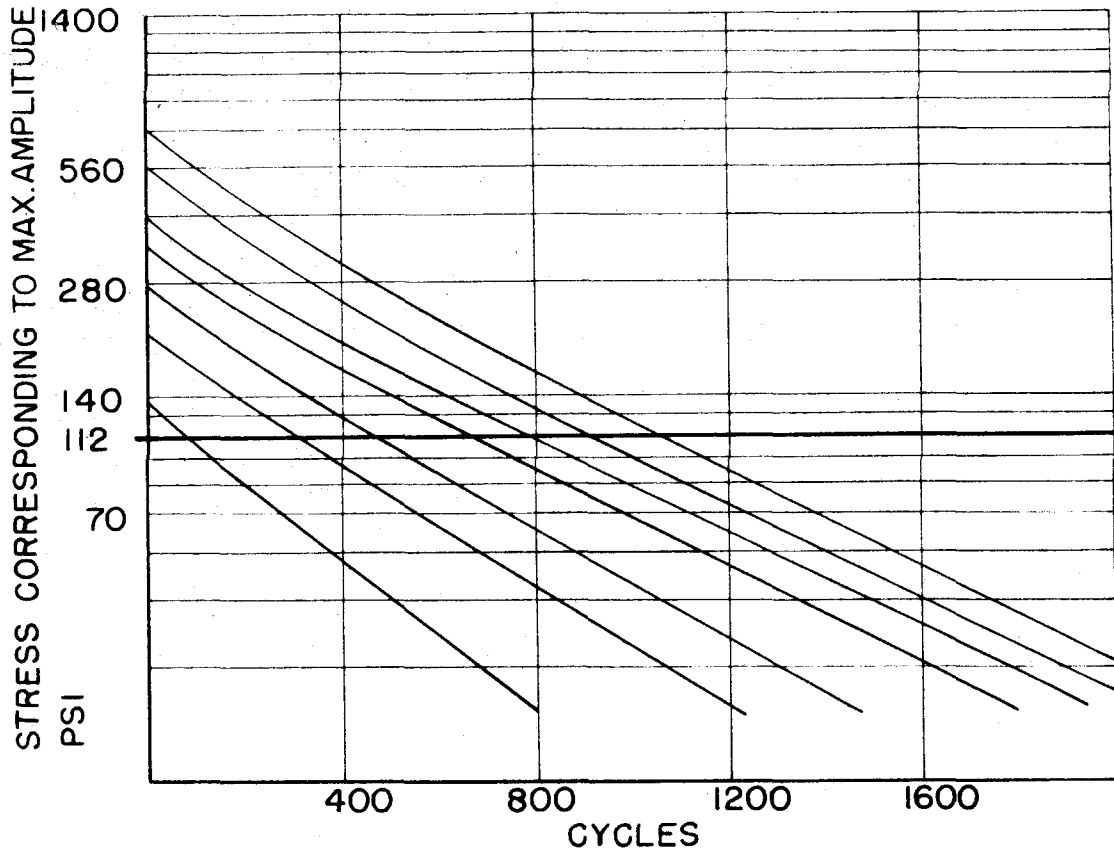


FIG. II - DAMPING CURVES FOR 350 ALUMINUM IN TORSION

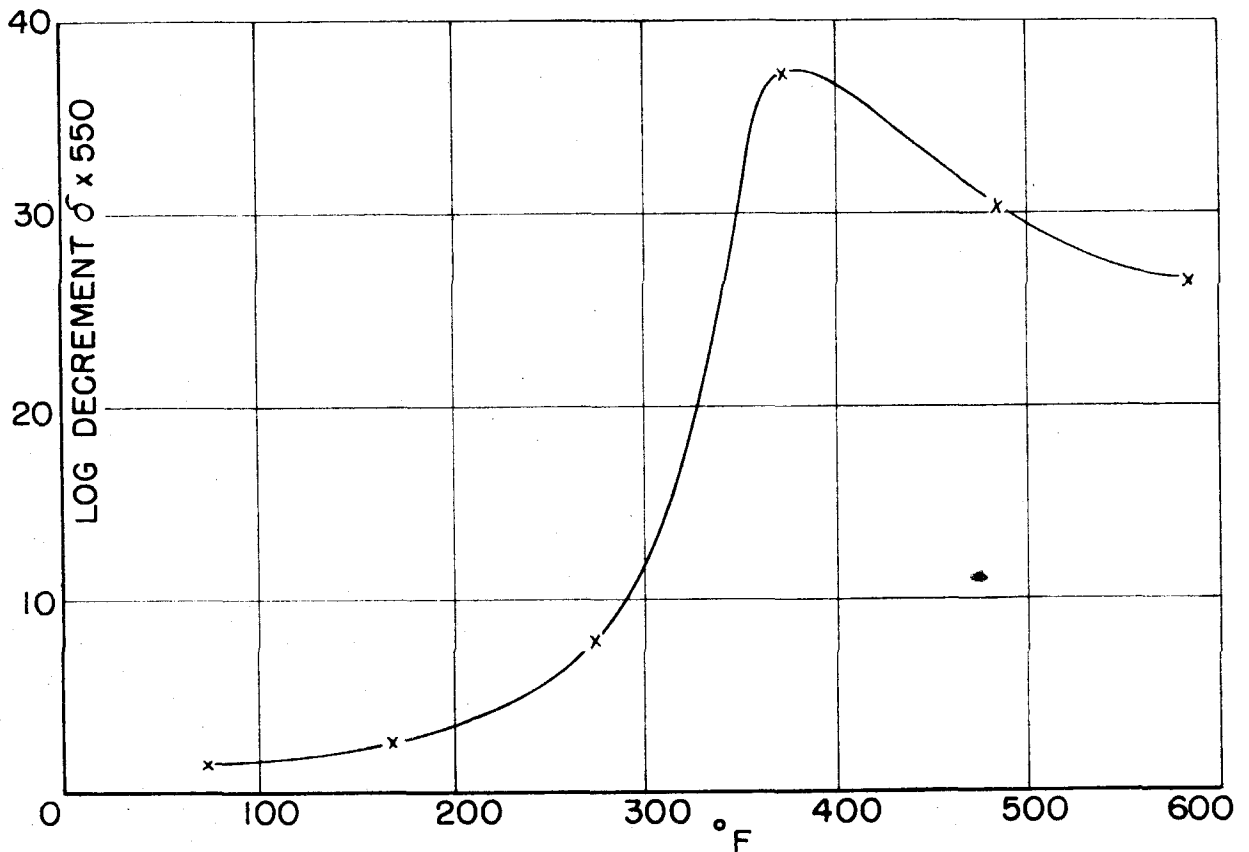


FIG. 12 - VARIATION OF INTERNAL FRICTION WITH TEMPERATURE

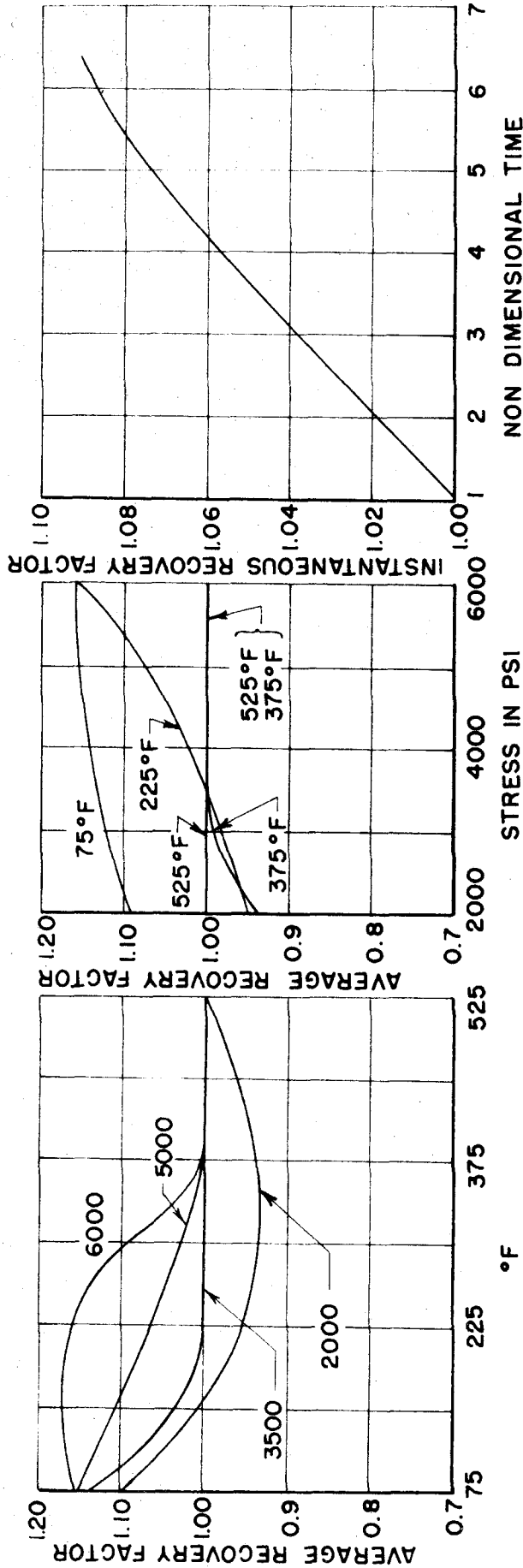


FIG.13 - VARIATION OF RECOVERY
FACTOR WITH TEMPERATURE
FOR VARIOUS PARAMETRIC
VALUES OF STRESS

FIG.14 - VARIATION OF RECOVERY
FACTOR WITH STRESS FOR
VARIOUS PARAMETRIC
VALUES OF TEMPERATURE

FIG.15 - RECOVERY IN A TYPICAL
CASE AS A FUNCTION OF
NON DIMENSIONAL TIME
CASE DATA : 2000-75-1
TAKEN AT 6.6×10^6 CYCLES

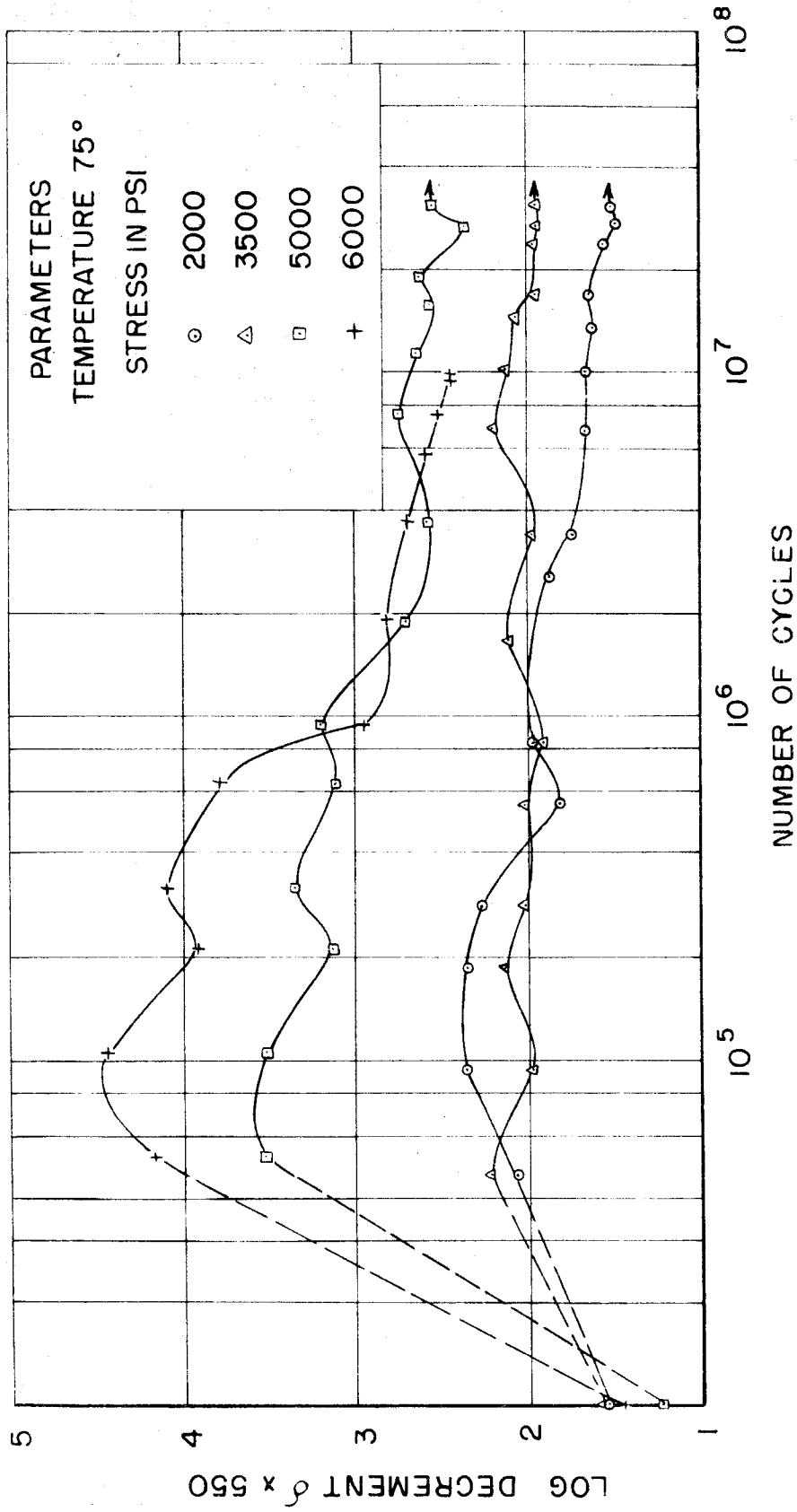


FIG. 16

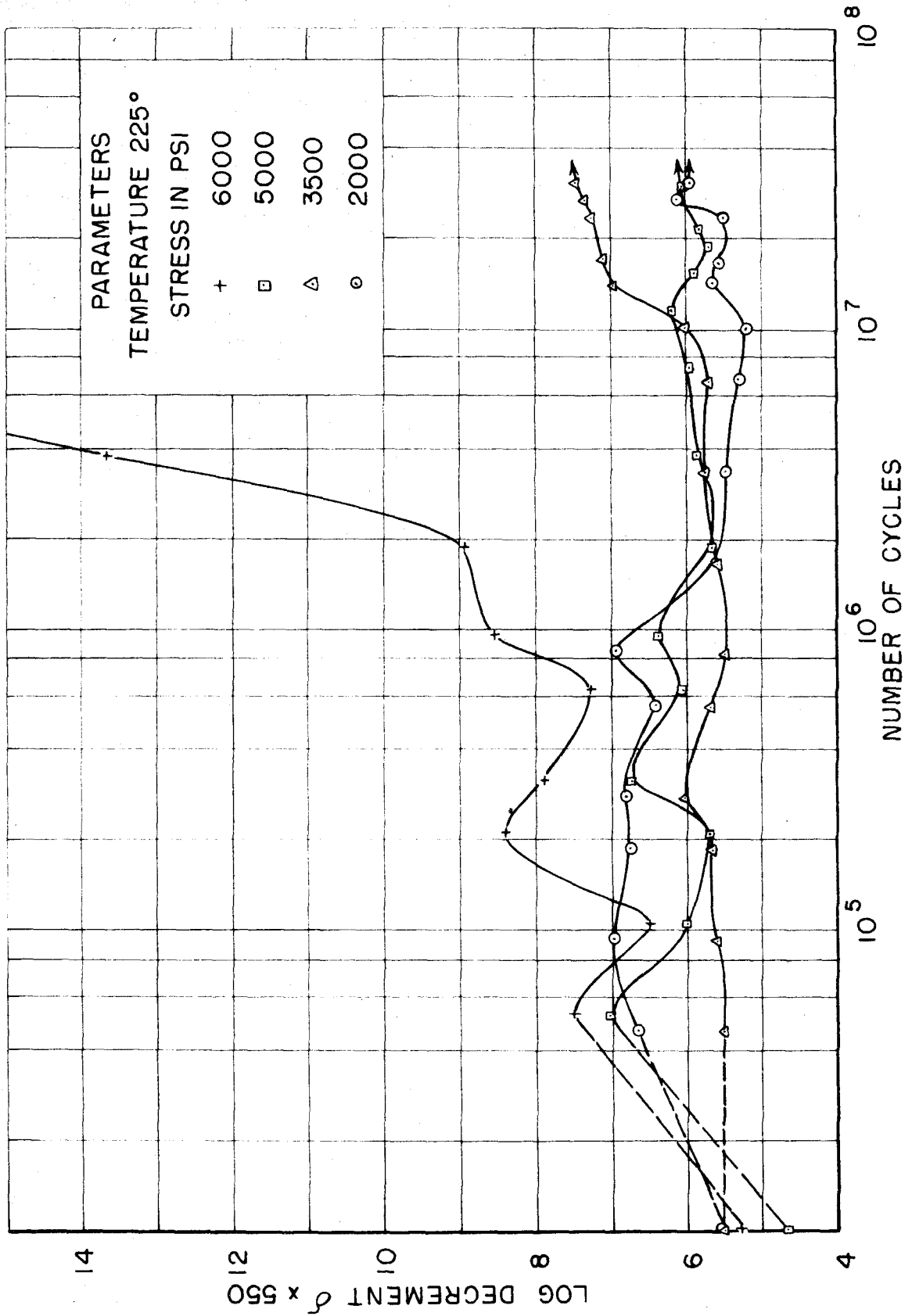


FIG. 17

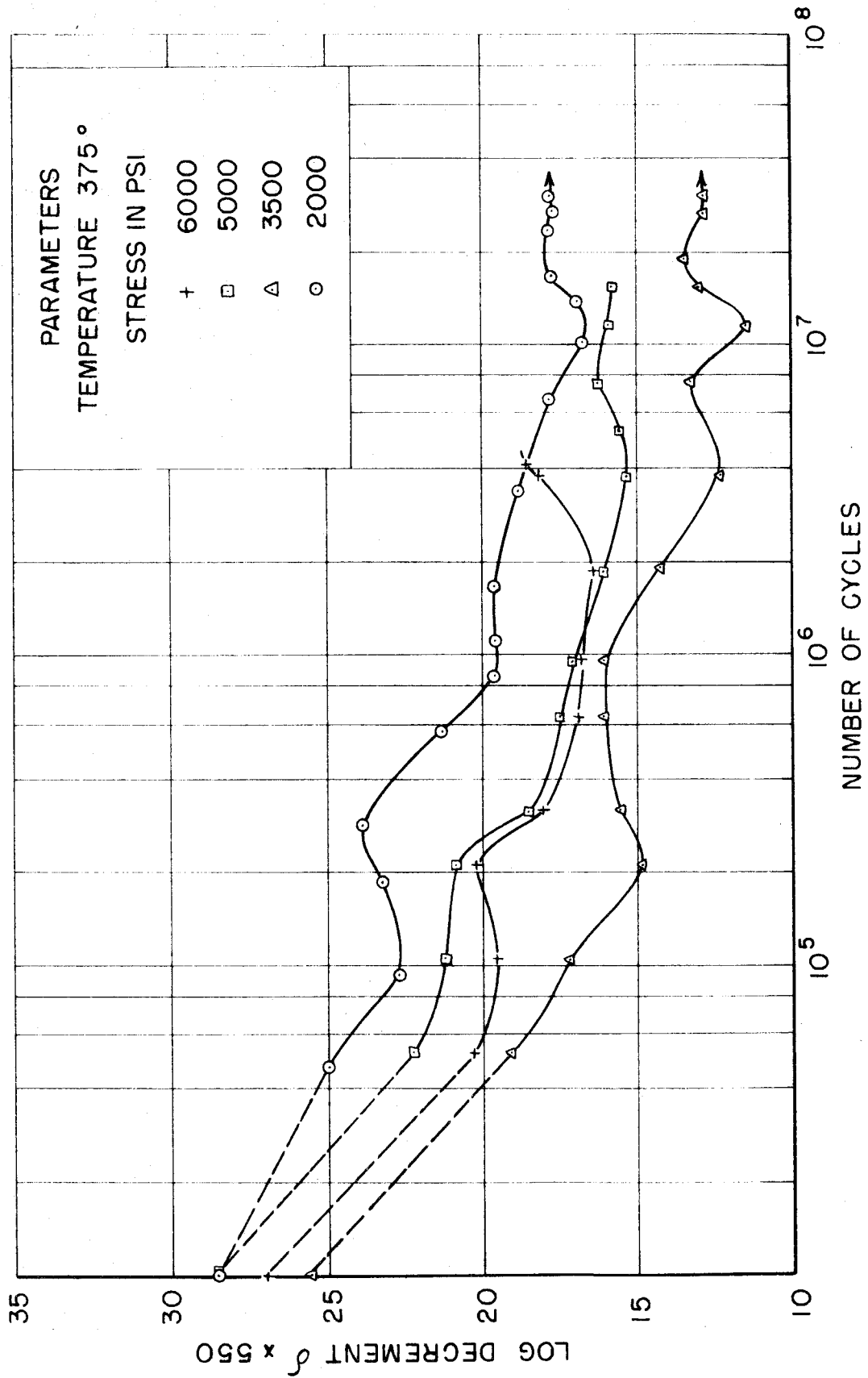


FIG. 18

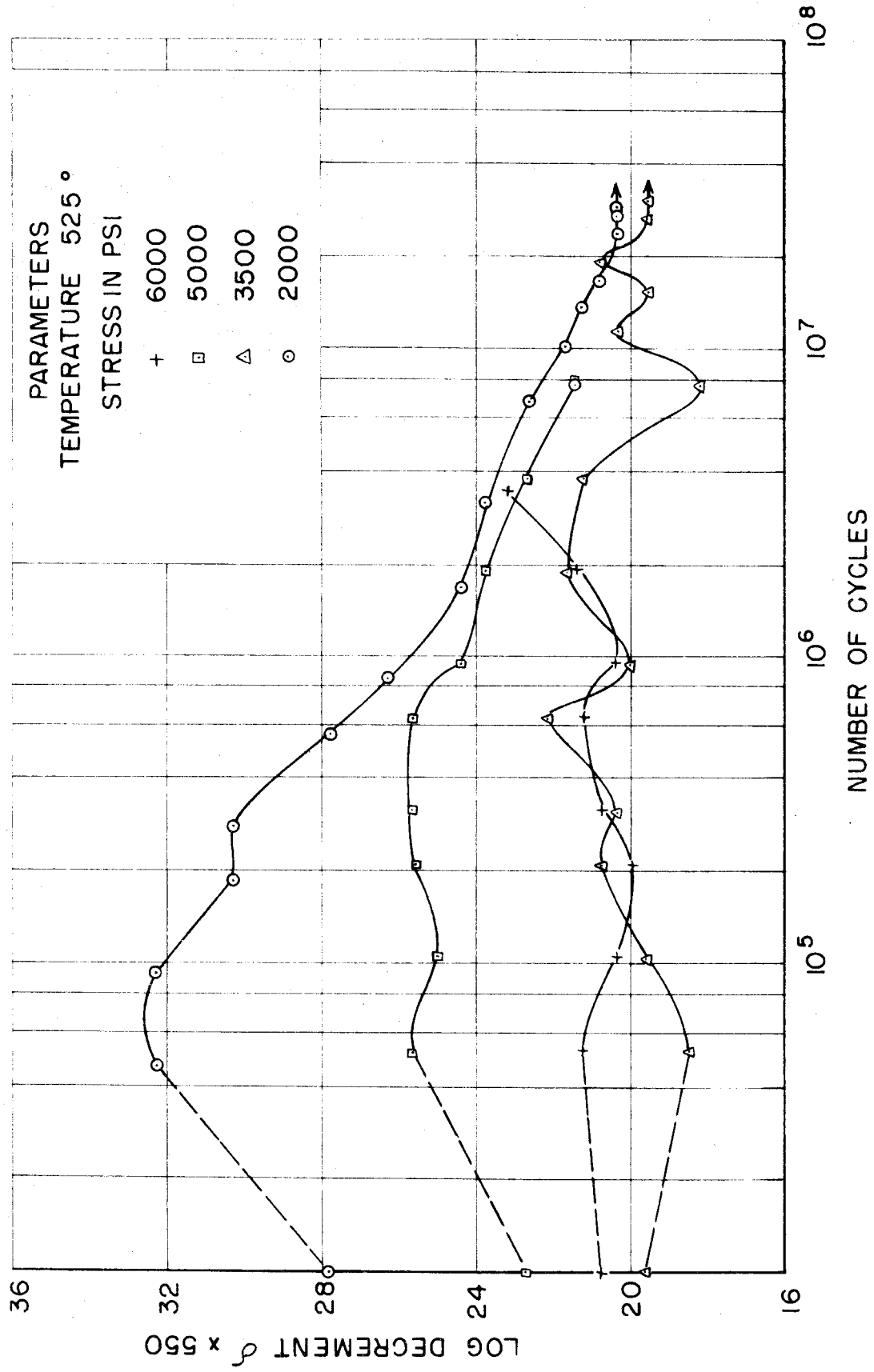


FIG.19

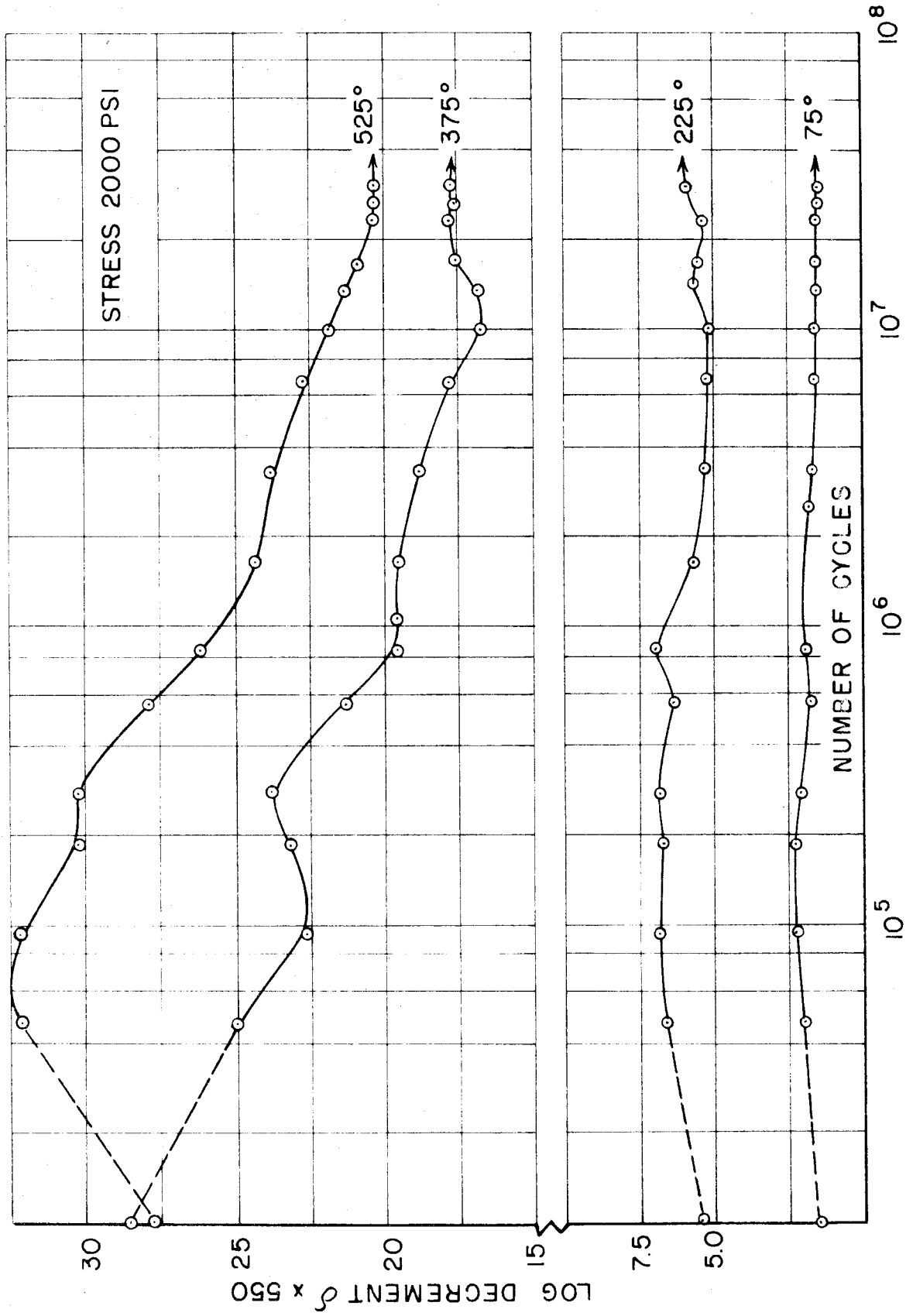


FIG. 20

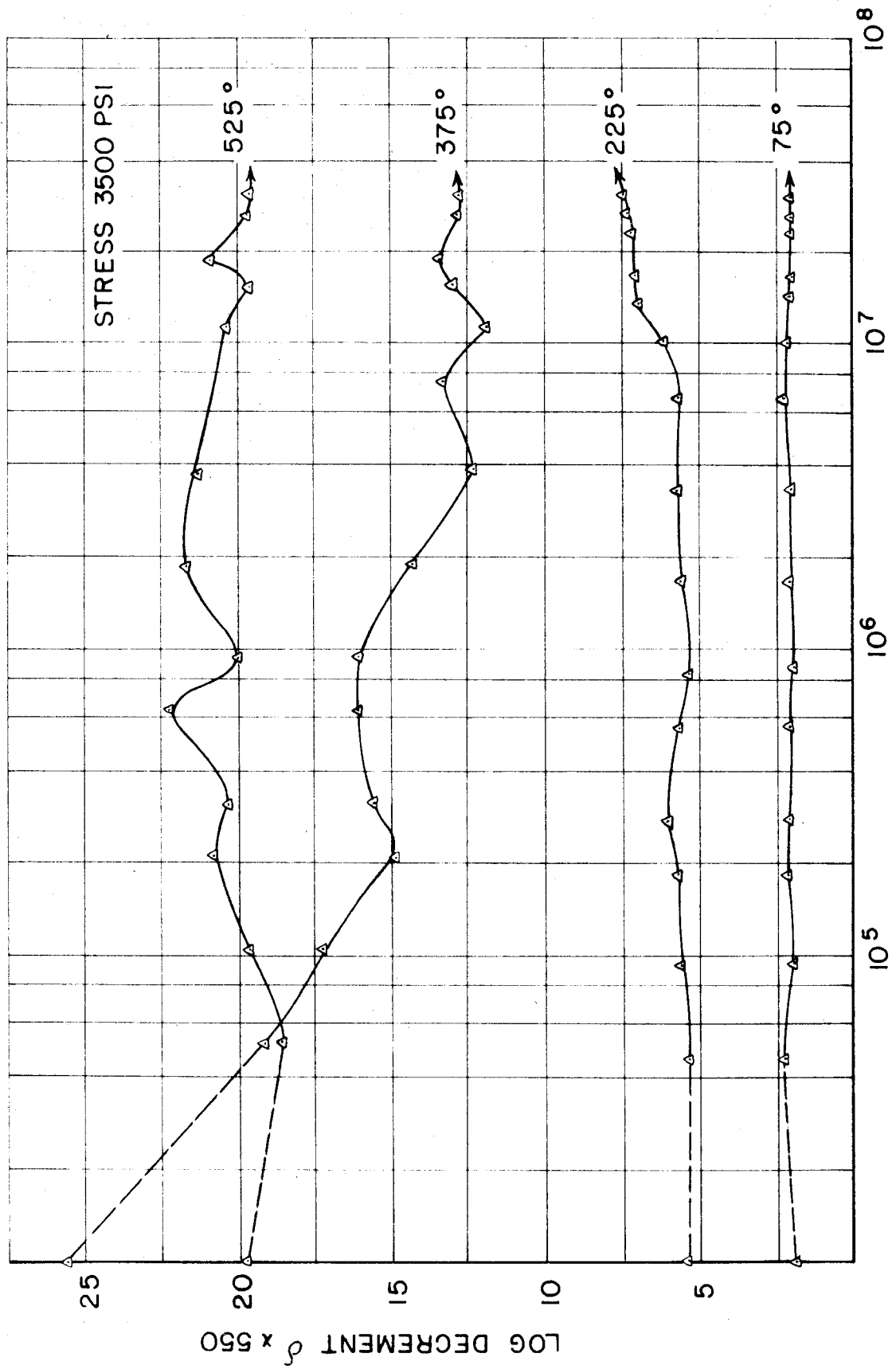


FIG. 21

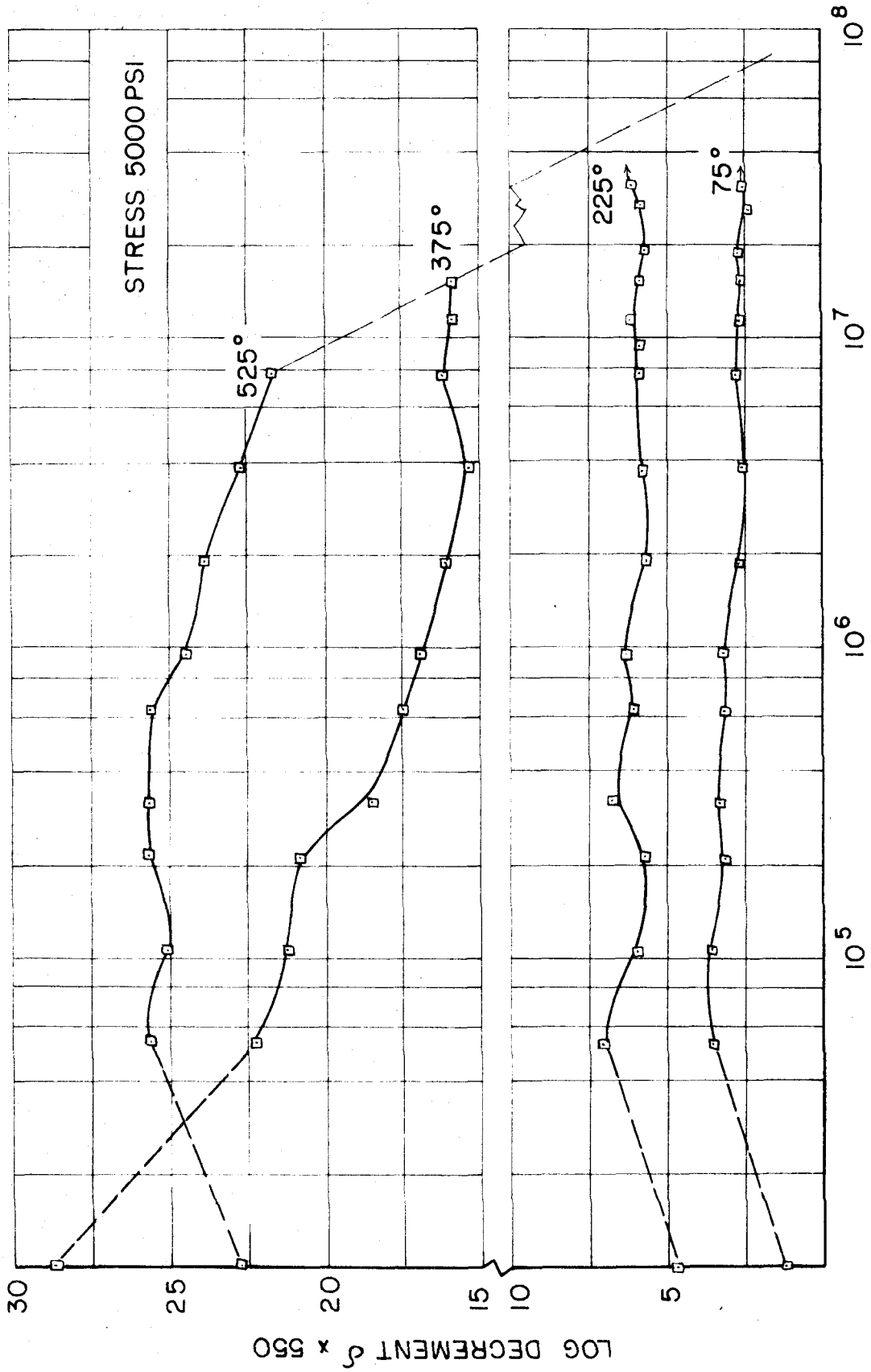


FIG. 22

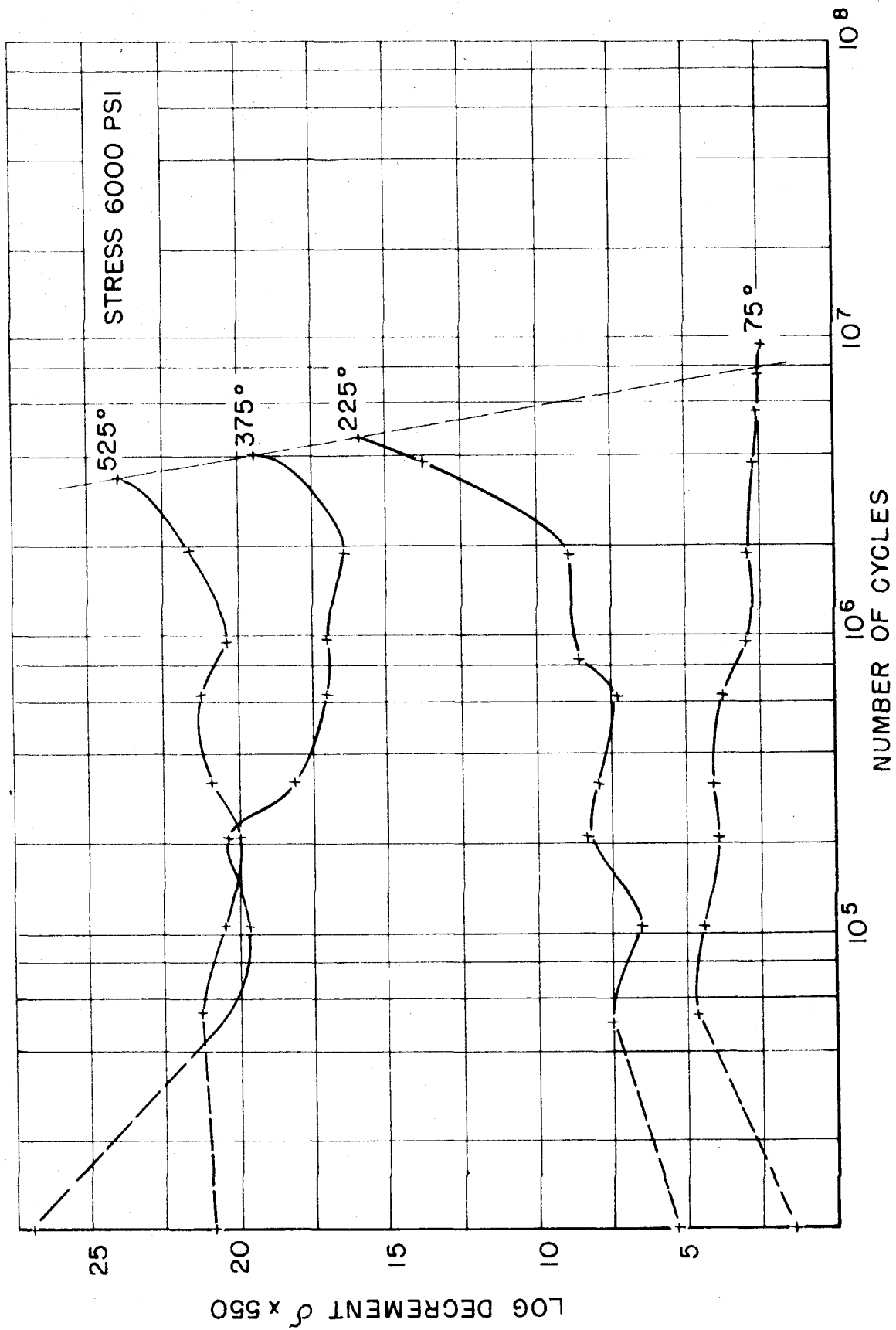


FIG. 23

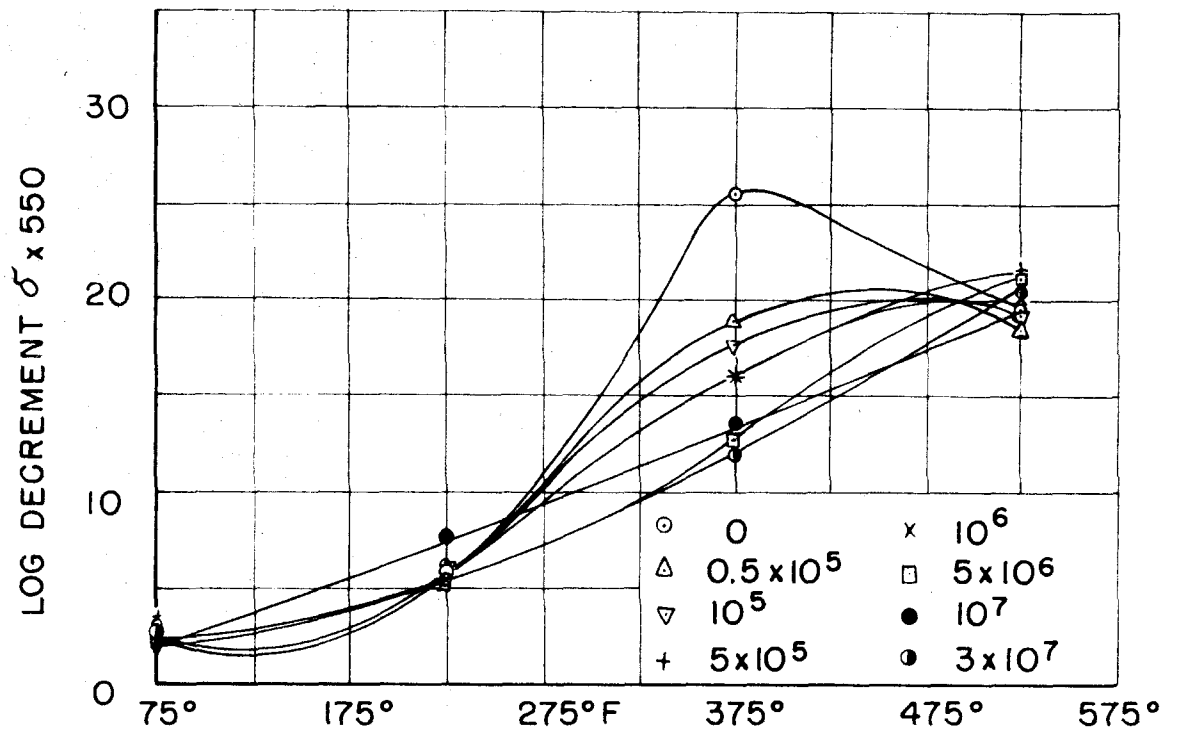


FIG. 24 - VARIATION OF σ WITH T AFTER APPLICATION OF FATIGUE STRESS 3500 PSI

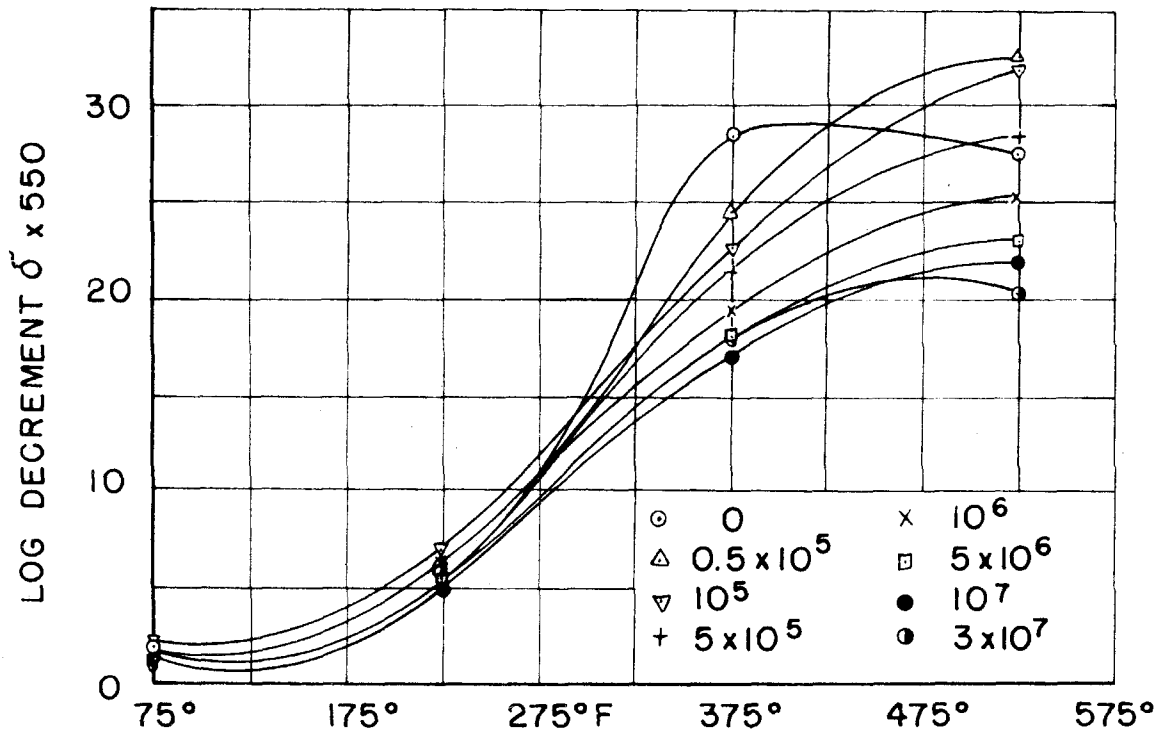


FIG. 25 - VARIATION OF σ WITH T AFTER APPLICATION OF FATIGUE STRESS 2000 PSI

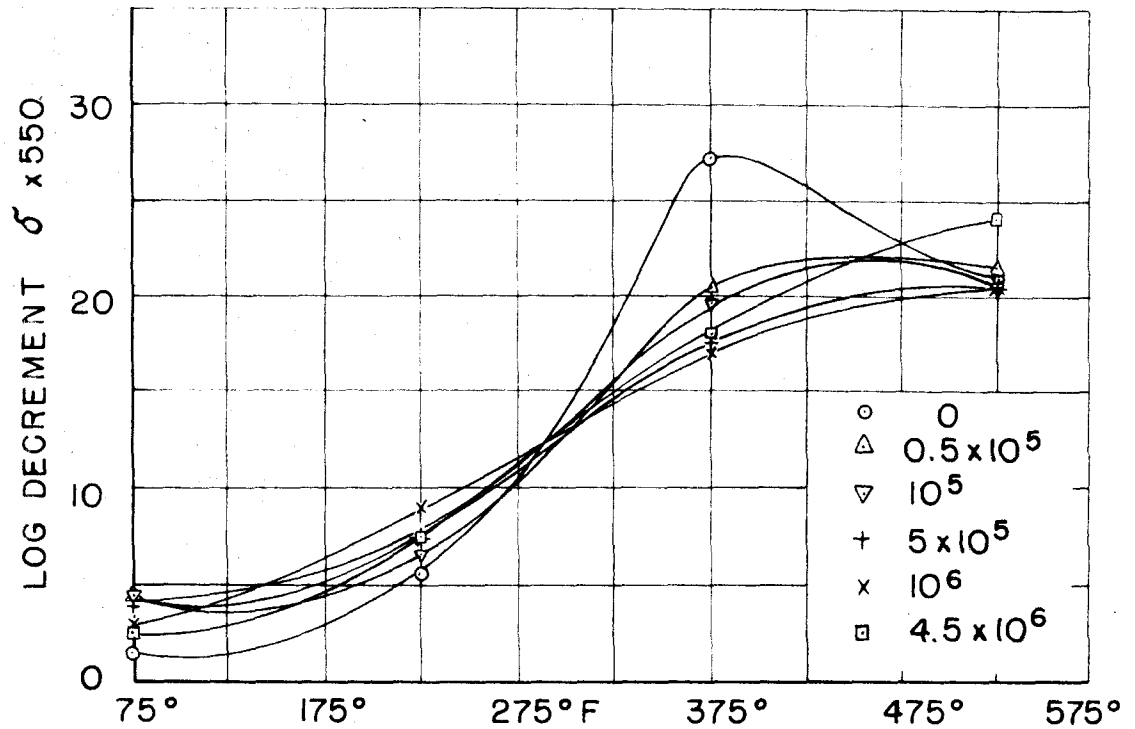


FIG.26-VARIATION OF σ WITH T AFTER APPLICATION OF FATIGUE STRESS 6000 PSI

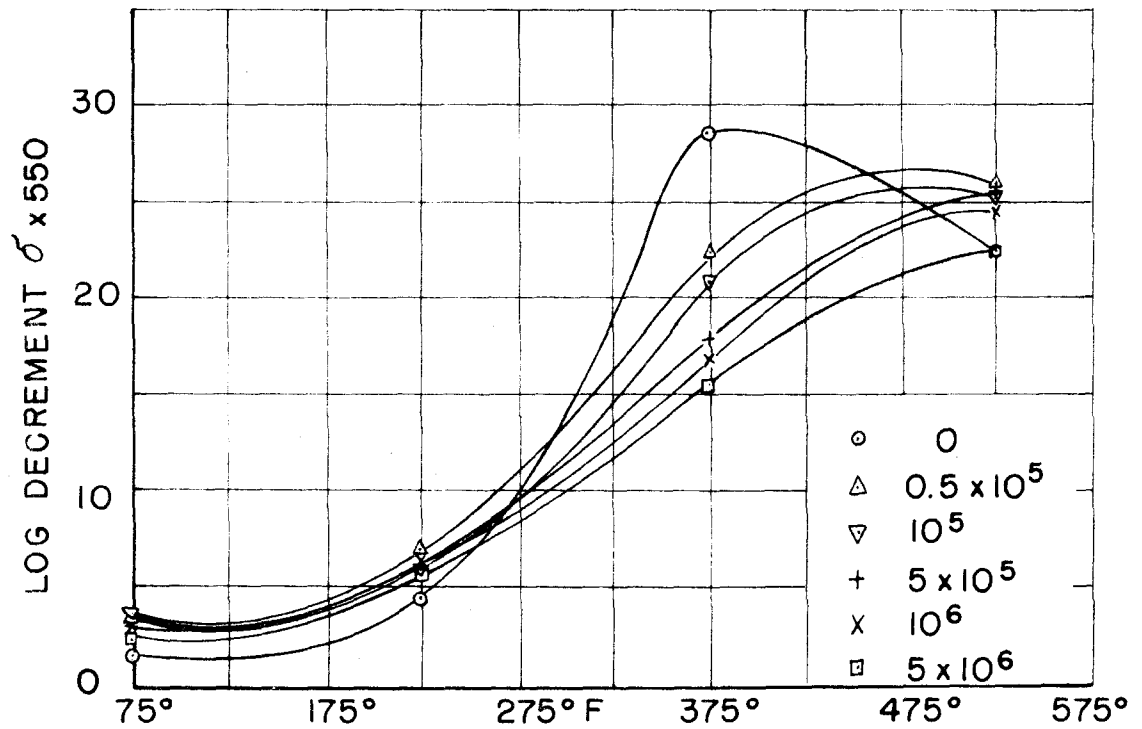


FIG.27-VARIATION OF σ WITH T AFTER APPLICATION OF FATIGUE STRESS 5000 PSI

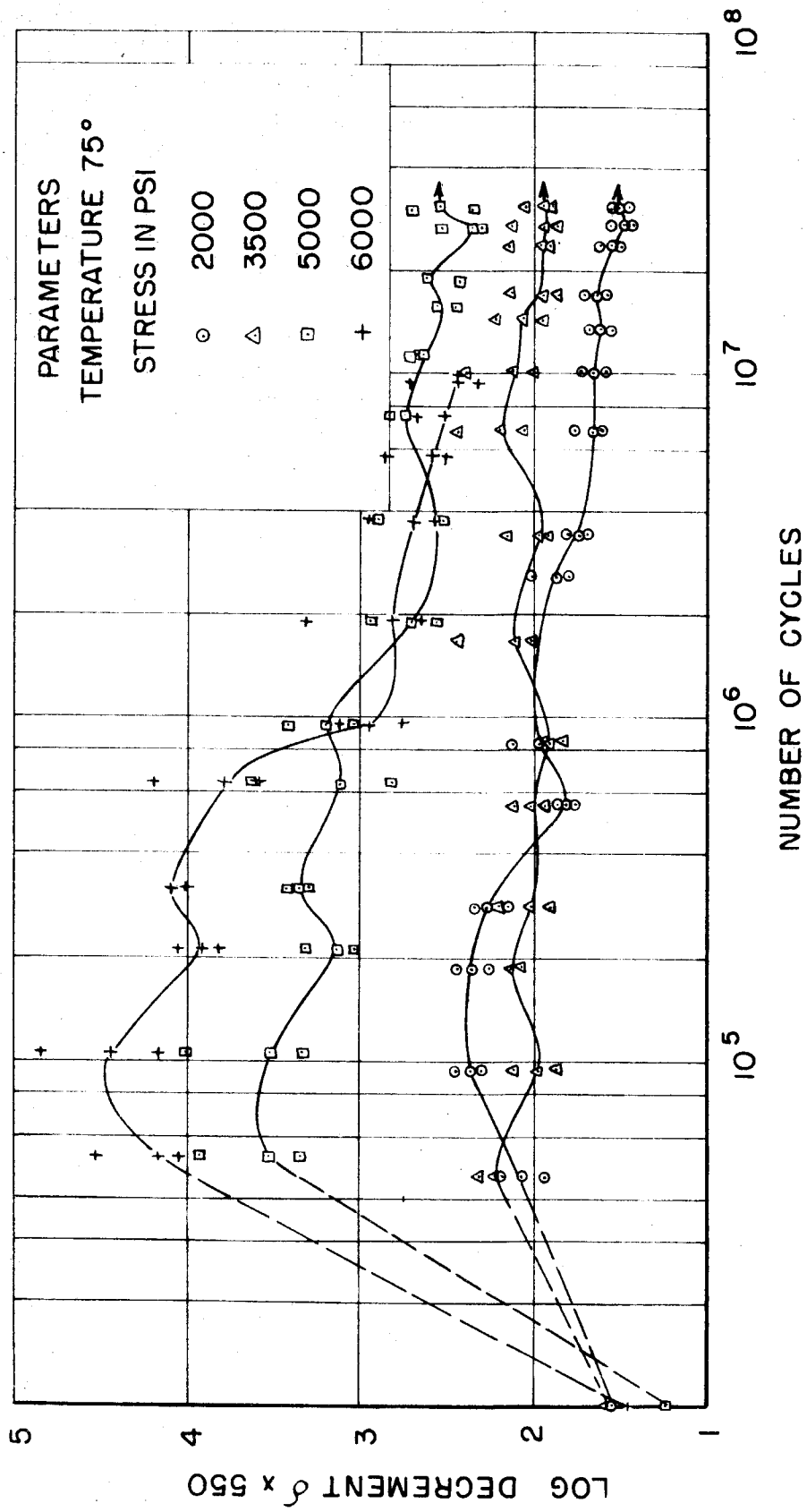


FIG. 28